AD _____

SARAH MELLON SCAIFE
RADIATION LABORATORY
UNIVERSITY OF PITTSBURGH
Pittsburgh, Pennsylvania

TECHNICAL REPORT NO. V
ON PRECISION SCATTERING AND OTHER RESEARCHES

March, 1953

OFFICE OF NAVAL RESEARCH
Contract N7onr---32505
Project Designation Number NR022-068

SARAH MELLON SCAIFE
RADIATION LABORATORY
UNIVERSITY OF PITTSBURGH
Pittsburgh, Pennsylvania

TECHNICAL REPORT NO. V

ON PRECISION SCATTERING AND OTHER RESEARCHES

OFFICE OF NAVAL RESEARCH
Contract N7onr—32505
Project Designation Number NR022-068

Radiation Laboratory

University of Pittsburgh

Pittsburgh, Pennsylvania

TECHNICAL REPORT NO. V

On Precision Scattering and Other Researches

Office of Naval Research

Navy Contract N7onr-32505

Project Designation Number NR022-068

ABSTRACT

This report is a compilation of reprints and articles of certain researches carried on at the Sarah Mellon Scaife Radiation Laboratory, The University of Pittsburgh.

TABLE OF CONTENTS

Reprinted from THE PHYSICAL REVIEW, Vol. 85, No. 1, 101-103, January 1, 1952
Printed in U. S. A.

Internal Conversion in Pr^{143}, In^{114}, Ba^{137}, and Cd^{110}*

W. C. KELLY
University of Pittsburgh, Pittsburgh, Pennsylvania†

(Received August 20, 1951)

Beta-ray spectrometer measurements have been made of the internal conversion ratio α_K/α_L for four nuclear transitions. Values obtained are: 5.3±0.1 for the 132 kev transition in Pr^{143}; 1.30±0.05, 192 kev, In^{114}; 4.57±0.05, 562 kev, Ba^{137}; and 14±2, 656 kev, Cd^{110}. Tentative assignments of multipolarity are given.

I. INTRODUCTION

FROM measurements of the conversion coefficient for the K shell or the ratio of the K conversion coefficient to the L conversion coefficient, one can, in principle, obtain the multipole order of nuclear transitions and hence the spin and parity changes needed to establish decay schemes. However, the only reliable values of conversion coefficients existent are the values of α_K calculated by Rose *et al.*[1] using exact relativistic wave functions for a wide range of energies, Z values, and multipole orders. Experimental determinations of α_K alone are difficult except when the decay scheme is known to be simple. A few methods have been proposed to obtain α_K for a gamma-ray emitted in a complex decay scheme by utilizing Compton scattering[2] or external conversion.[3] In addition to the experimental difficulty, one faces the possibility that the interpretation of values of α_K may be ambiguous if mixtures of electric 2^l-pole and magnetic $2^{l\pm1}$-pole processes occur in nuclides of low Z.[4] Therefore, one would prefer to measure α_K/α_L and from the ratio to obtain an unambiguous assignment of multipolarity. For the interpretation, the experimentalist will have to await the exact calculation of the L conversion coefficient, which is reported[1] to be under way. Meanwhile, approximate calculations are available for tentative assignments.[5-7]

In this experimental study, beta-ray spectrometer measurements were made of the ratio of α_K/α_L for gamma-rays emitted by the nuclides praseodymium 144, indium 114, barium 137, and cadmium 110.

II. EXPERIMENTAL

Quade and Halliday[8] have described the construction and electron optical properties of the magnetic lens beta-ray spectrometer used in these studies. Additional precautions were taken in the present work to reduce scattering within the chamber and alignment errors. Antiscattering baffles were installed near the source and near the counter. The interior of the spectrometer was covered with a rough coating of ceresin wax. A simple experiment showed that this wax reduces electron scattering by a factor of at least two. It was found necessary to locate the central baffle quite accurately so that the annular aperture at the center of the spectrometer would be uniformly wide. Failure to do this led to a broadening of internal conversion lines.

For this work, a thin-window Geiger counter was developed in which the beta-particles entered at right angles to the axis of the counter. Such a counter has the advantages that both ends of the central wire are accessible for flashing the wire and that the sensitive volume of the counter extends to the window. The counter showed a long term stability, a flat plateau (1.6 percent per 100 volts), and a low background (30 counts/minute). The window had an areal density of 30 μg/cm^2 and transmitted electrons to energies as low as 5 kev.

Three of the four radioactive materials were available at reasonably high specific activities. Cesium 137, the parent of barium 137, was obtained from Oak Ridge as cesium chloride at an activity of 1.05 mC/ml and with total solids not exceeding 2.4 mg/ml. Cerium 144 was obtained there also as cerium nitrate (3.06 mC/ml and 1.8 mg/ml). Indium 114 was produced in the University of Pittsburgh cyclotron by a $Cd^{114}(d,n)$ reaction and cleanly separated at the radiochemistry laboratory of the Atomic Power Division, Westinghouse Electric Corporation, by H. A. Brightsen. Silver 110, produced at Oak Ridge by neutron bombardment, had a low specific activity (3.97 mC/ml and 150 mg/ml). The thick source resulting from the low specific activity caused difficulty in resolving the cadmium 110 conversion lines. The sources were prepared by depositing a minimal amount of the concentrated radioactive solution upon an aluminum backing of thickness 0.00025 inch. Average areal densities of the sources were obtained by weighing. The areal density of the cerium, indium, and cesium sources was about 0.1 mg/cm^2. That of the silver source was 10 mg/cm^2.

Data were taken automatically.[9] Enough counts were recorded that the statistical error associated with each

* Part of a dissertation submitted in partial fulfillment of the requirements for the degree of Doctor of Philosophy at the University of Pittsburgh.

† Assisted by the joint program of the AEC and ONR and by the Research Corporation.

[1] Rose, Goertzel, Spinrad, Harr, and Strong, Phys. Rev. **83**, 79 (1951).

[2] K. Siegbahn, Proc. Roy. Soc. (London) **189**, 541 (1946).

[3] C. D. Ellis and G. Aston, Proc. Roy. Soc. (London) **129**, 180 (1930).

[4] P. Axel and R. F. Goodrich, Navy Report "Internal conversion data," privately circulated.

[5] M. H. Hebb and E. Nelson, Phys. Rev. **58**, 486 (1940).

[6] N. Trallі and I. S. Lowen, Phys. Rev. **76**, 1541 (1949).

[7] S. D. Drell, Phys. Rev. **75**, 132 (1949).

[8] E. A. Quade and D. Halliday, Rev. Sci. Instr. **19**, 234 (1948).

[9] W. C. Kelly and K. J. Metzgar, Rev. Sci. Instr. **22**, 665 (1951).

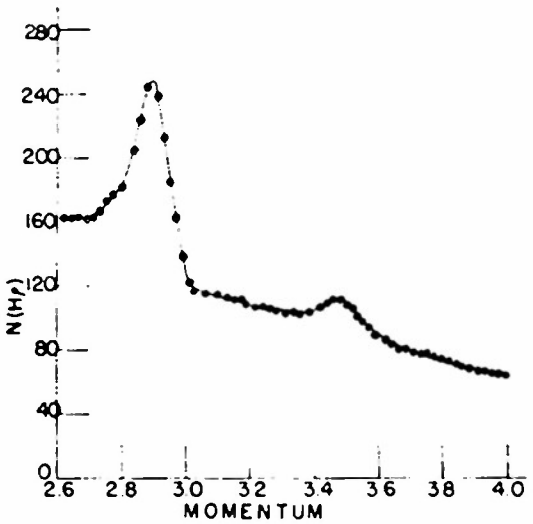

FIG. 1. The electron spectrum of $Ce^{144}-Pr^{144}$ in the region of the conversion peaks of the 132-kev gamma ray of Pr^{144}. $N(H\rho)$, the number of electrons per unit time per unit momentum interval, is plotted against the electron momentum in arbitrary units.

experimental point did not exceed two percent except where the curves approached the background level.

III. RESULTS

A. Praseodymium 144

A portion of the electron spectrum of cerium 144-praseodymium 144 is shown in Fig. 1. To obtain the conversion peaks of the gamma-ray at 132 kev, it was necessary to subtract the continuous spectrum from the total curve. This was done by making a Fermi plot for cerium and with its help reconstructing the continuous spectrum at the conversion peaks. By subtraction of the continuous spectrum, the conversion peaks of Fig. 2 were obtained. The spread of the K peak is 4 percent. The low energy portion of each line is approximately exponential, a measure of the degradation of the energy of the electrons as they leave the source. In addition to the experimental evidence of Fig. 2, there seems to be theoretical justification[10] for regarding this portion of the curve as exponential. An exponential curve has been fitted to the K peak to extend it to the momentum axis through a region of the total curve where other conversion lines are present. An exponential curve fitted to the L peak extended it to the momentum axis. The correction to the high energy side of the K peak was negligible. The ratio of the areas under the peaks gave $\alpha_K/\alpha_L=5.3\pm0.1$.

The converted gamma-ray must be ascribed to praseodymium 144. Best agreement for the energy of of the gamma-ray is obtained by adding to the energies of the K and L conversion electrons the binding energies for praseodymium. Critical absorption experiments were carried out using aqueous solutions of barium and cesium as absorbers. The absorption data showed conclusively the presence of x-rays which could be either praseodymium $K\alpha$ or neodymium $K\alpha$. Energy considerations make it likely that it is the former. This assignment agrees with that by Emmerich *et al.*[11]

The experiment value of 5.3 ± 0.1 for α_K/α_L indicates an electric quadripole radiation if one uses the non-relativistic calculations of Hebb and Nelson.[5] Their results give the following conversion ratios: E 2^1 pole, 8.4; E 2^2-pole, 4.5; E 2^3-pole, 1.2. Emmerich *et al.*[11] report an approximate value of 7 for α_K/α_L.

B. Indium 114

Conversion peaks for the 192-kev gamma-ray of metastable indium 114 are shown in Fig. 3. The spread is 3.3 percent. The contribution of the 2.05-Mev beta-group to the electron intensity at this energy is negligible.

Separation of the two peaks for purposes of planimetry was effected by a method involving successive approximations to the separate curves. First, a gaussian curve[12] was fitted to the high energy side of the K peak. By subtracting this curve from the total curve between the two peaks, one could decide how to continue the L peak in an exponential. The exponential portion of the L peak was then subtracted from the total curve to give a second approximation to the high energy portion of the K peak.

α_K/α_L was found to be 1.30 ± 0.05 and indicates either an electric 2^4-pole or an electric 2^5-pole transition.

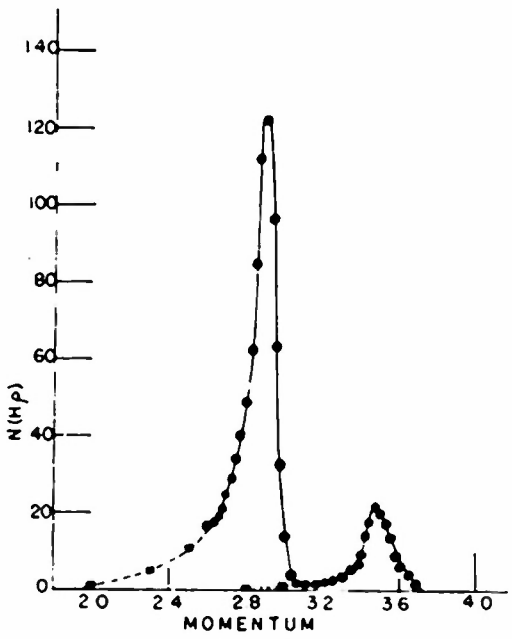

FIG. 2. The conversion electrons of the 132 kev gamma-ray of Pr^{144}. Circles show the experimental points, squares show points on the calculated exponential curves.

[10] G. E. Owen, private communication.

[11] Emmerich, John, and Kurbatov, Phys. Rev. 82, 968 (1951).

[12] The line shape of a magnetic lens spectrometer can be approximated quite well by a skewed gaussian curve. See Van Atta, Warshaw, Chen, and Taimaty, Rev. Sci. Instr. 21, 985 (1950).

Hebb and Nelson give the following values: E 2^4-pole, 1.7; E 2^5-pole, 0.9. Lawson and Cork[13] report a value of 1.0 ± 0.1 for α_K/α_L. Boehm and Preiswerk[14] give 1.1 ± 0.1, and Steffen[15] reports 1.10 ± 0.05.

C. Barium 137

Figure 4 shows the K and $L-M$ conversion peaks of the 662-kev gamma-ray of metastable barium 137. The spread of the K line is 1.4 percent. A value of 4.57 ± 0.05 is found for $\alpha_K/\alpha_{L,M}$ in good agreement with the result $\alpha_K/\alpha_{L,M}=4.54$ obtained by Langer.[16] Mitchell and Peacock[17] report the value 4.8 for α_K/α_L, and Osoba[18] finds $\alpha_K/\alpha_L=5.0$. Tentatively, one may assign a multipolarity of electric 2^5 to the transition. It must be emphasized, however, that the nonrelativistic theory may be considerably in error at this energy.

D. Cadium 110

Cadmium 110 is the daughter nucleus by negatron emission of silver 110. The K and $L-M$ conversion peaks of the 656-kev gamma-ray of cadmium 110 have been measured with a line spread of 3.7 percent. The peaks were separated by the procedure referred to above. However, a correction must be applied to the $L-M$ peak to correct for the presence of K conversion electrons due to a gamma-ray of energy 676 kev whose K peak is superimposed (within 2 kev) upon the $L-M$ peak of the 656-kev gamma-ray. The 676-kev line was discovered by Siegbahn[19] in studying the photoelectron spectrum of these radiations in a lead converter. Three lines in the spectrum (676 kev, 705 kev, 759 kev) have about the same photoelectric intensities. Siegbahn concludes that the gamma-intensities are probably about the same upon the assumption that the lines are of the same multipole order. On this basis, the conversion coefficient should be approximately the same, and the K peak of the 706-kev line should approximate that of the 676-kev line. The K peak of the 706-kev line can be readily measured. After applying this plausible, although certainly not rigorous, correction, $\alpha_K/\alpha_{L,M}$ was found to be 14 ± 2.

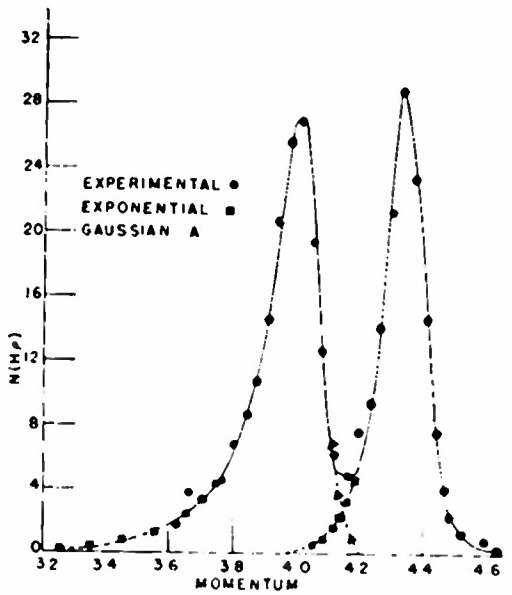

FIG. 3. The conversion electrons of the 192 kev gamma ray of Ir^{193}.

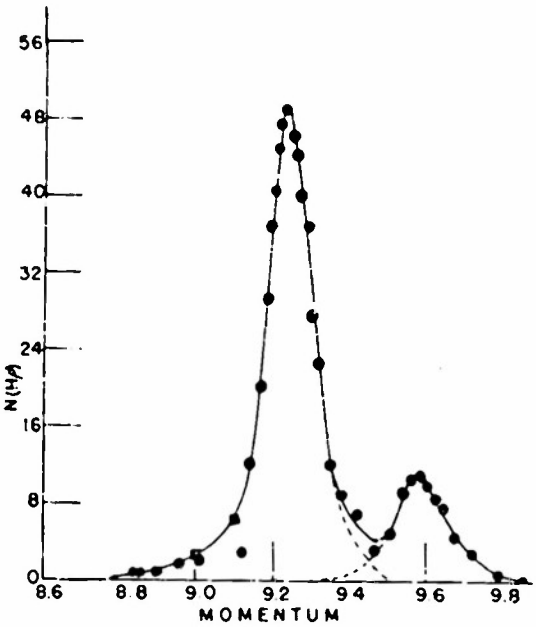

FIG. 4. The conversion electrons of the 662 kev gamma ray of Ba^{137}. Circles show the experimental points, squares show points on the calculated curves.

This result indicates electric dipole radiation according to the calculations of Hebb and Nelson. However, the difficulties introduced by the source thickness, the approximate nature of the correction for the interfering line, and the nonrelativistic theory used reduce the certainty of the assignment.

By two independent means, Siegbahn[19] has found α_K for this line to be 2.5×10^{-3}. The precise theory shows that this is consistent with either electric or magnetic dipole radiation.

The author would like to acknowledge the support and encouragement given him by Drs. D. Halliday, A. J. Allen, and G. E. Owen. Mr. Kenneth Metzgar assisted with the instrumentation. Mr. Samuel Broder prepared tables of the Fermi function.

[13] J. L. Lawson and J. M. Cork, Phys. Rev. **57**, 982 (1940).
[14] F. Boehm and P. Preiswerk, Helv. Phys. Acta **22**, 331 (1949).
[15] R. M. Steffen, Phys. Rev. **83**, 166 (1951).
[16] L. M. Langer, private communication.
[17] A. C. G. Mitchell and C. L. Peacock, Phys. Rev. **75**, 197 (1949).
[18] J. S. Osoba, Phys. Rev. **76**, 345 (1949).
[19] K. Siegbahn, Phys. Rev. **77**, 233 (1950).

Reprinted from THE PHYSICAL REVIEW, Vol. 85, No. 6, 857-859, June 15, 1952
Printed in U. S. A.

Nuclear Energy Levels of Al^{27}†

E. M. REILLEY,* A. J. ALLEN, J. S. ARTHUR, R. S. BENDER, R. L. ELY,‡ AND H. J. HAUSMAN
University of Pittsburgh, Pittsburgh 13, Pennsylvania

(Received February 18, 1952)

Twenty energy levels in Al^{27} have been found by the magnetic analysis of inelastically scattered protons at 90° from thin targets of aluminum. An analyzed beam of 8.0 Mev protons was utilized for the bombardment. Tentative values for the levels found are 0.844, 1.016, 2.259, 2.782, 3.036, 3.736, 4.018, 4.115, 4.473, 4.575, 4.647, 4.875, 4.996, 5.107, 5.220, 5.341, 5.501, 5.565, 5.620, 5.736 Mev. A broad alpha particle group from the $Al^{27}(p,\alpha)Mg^{24}$ reaction corresponding to an excited state of Mg^{24} was also observed and is believed to be complex.

INTRODUCTION

WILKENS and Kuerti[1,2] were the first to report on the measurement of the energy levels of aluminum by observation of inelastic scattering of protons. Since then, additional studies of this same nucleus have been made by several observers both by inelastic scattering experiments[3-8] and by other nuclear reactions.[9,10] In the experiment to be described, a large magnetic spectrometer was utilized for the measurement of energy of charged particles emitted from an aluminum foil target bombarded with a beam of magnetically analyzed 8-Mev protons.

APPARATUS

Details of the apparatus have been published elsewhere.[11] The proton beam was produced by the 47-inch University of Pittsburgh cyclotron. A large focusing magnet, placed about seven feet from the cyclotron vacuum tank, focused the beam on the entrance slits of a beam analyzer magnet which was located in an adjacent room. An eight-foot thick shielding wall separated this room from the cyclotron chamber. After traversing the beam analyzer field the beam was limited by stops to an angular extent of ±3 degrees horizontally and passed through a final analyzer slit, $\frac{1}{16}$ inch wide and $\frac{7}{8}$ inch high which limited the beam energy spread to 20 kev. Targets were placed at the center of a large scattering chamber at a distance of 1.75 inches from the final beam analyzer slit.

A large 60°-sector magnetic spectrometer was positioned at an angle of 90° with respect to the beam center. Charged particles emitted from the target were focused by this magnetic lens on a scintillation screen mounted external to the vacuum system. A 0.1-mil nickel foil served as the window. Stops were provided to limit the angular aperture to ±2° with respect to the center line of the system.

Field excitation currents for the three magnets were obtained from motor-generator sets which were electronically stabilized. The magnetic field of the beam focusing magnet was adjusted so as to yield maximum beam on the entrance slit of the beam analyzer. The magnetic fields in the beam and particle analyzers were measured by means of the proton magnetic resonance method[12] to one part in 10,000 and were continuously monitored during the experiment. Target beam currents of 0.5 to 1.0 microamperes were obtained.

In order to provide uniform bombardments, an insulated Faraday cup was placed behind the target so as to collect the beam. This cup was connected to a precharged polystyrene condenser, the potential of which was monitored by means of a Lindeman-Ryerson electrometer. A switching arrangement was provided so as to permit termination of the counting period when the electrometer indicated zero potential.

Scintillation counters consisting of a phosphor screen and either an RCA type 5819 or an EMI 5311 photomultiplier tube were used as particle detectors. Rather thick layers of silver-activated zinc sulfide deposited on glass slides from alcohol-water suspensions were found to be satisfactory for initial survey work. These had adequate sensitivity for both alpha-particles and protons and yet were comparatively insensitive to the gamma-ray background. Thin deposits of this same phosphor were found to be useful in obtaining discrimination in counting alpha-particles in the presence of undesired protons. A selsyn-controlled absorption-foil shutter was mounted immediately in front of the scintillation screen so that alpha-particles could be stopped when desired. This shutter carried a number of aluminum foils of different thickness. Pulses from the photomultiplier tube were fed by a cathode follower through a long matched coaxial line to a separate room and further amplified by a Jordan and Bell type linear

† Work done in the Sarah Mellon Scaife Radiation Laboratory and assisted by the joint program of the ONR, AEC, and the Research Corporation.

* Now at Camp Evans Signal Laboratories, Belmar, New Jersey.
‡ Now at Westinghouse Atomic Power Division, Bettis Field, Pittsburgh, Pennsylvania.

[1] T. R. Wilkens, and G. Kuerti, Phys. Rev. **57**, 1082 (1940).
[2] T. R. Wilkens, Phys. Rev. **60**, 365 (1941).
[3] R. H. Dicke and J. Marshall, Phys. Rev. **59**, 914 (1941).
[4] E. M. Hafner, Ph.D. thesis, University of Rochester, 1948.
[5] E. H. Rhoderick, Proc. Roy. Soc. (London) **201**, 348 (1950).
[6] Reelley, Sampson, and Mitchell, Phys. Rev. **76**, 624 (1949).
[7] H. W. Fulbright and R. R. Bush, Phys. Rev. **74**, 1323 (1948).
[8] K. K. Keller, Phys. Rev. **84**, 884 (1951).
[9] Swann, Mandeville, and Whitehead, Phys. Rev. **79**, 508 (1950).
[10] VanPatter, Sperduto, and Enge, Phys. Rev. **83**, 212 (1951).
[11] Bender, Reilley, Allen, Ely, Arthur, and Hausman, Rev. Sci. Instr. (to be published).
[12] R. V. Pound and W. D. Knight, Rev. Sci. Instr. **21**, 219 (1950).

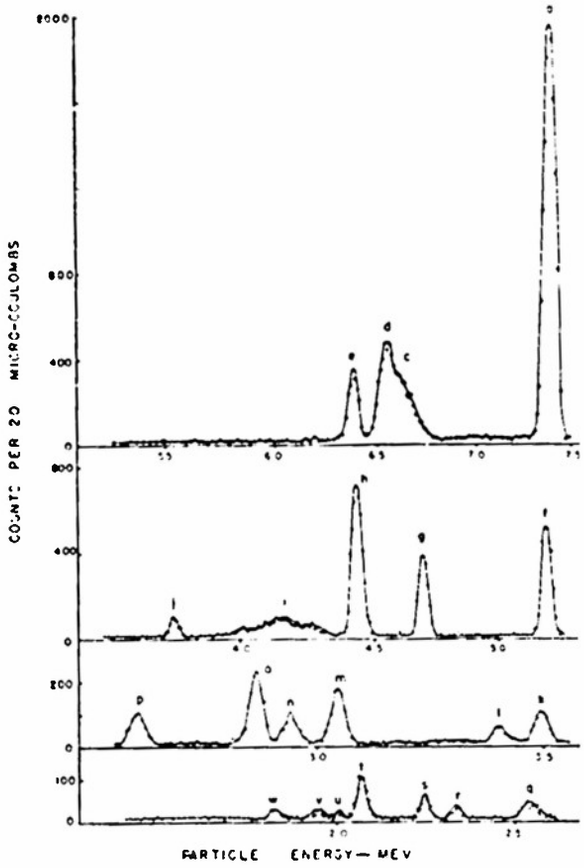

FIG. 1. Spectrum of magnetically analyzed particles obtained at 90° and Al^{27} bombarded by 8-Mev protons.

amplifier. The amplified pulses were fed into three pulse-height discriminators, each set at a different level and each connected to a separate scaling circuit. This counting arrangement permitted crude pulse-height analysis to be made and indicated whether protons, deuterons, or alpha-particles were being counted during initial searches for charged particle groups.

CALIBRATION

The spectrometer was calibrated by using alpha-particles from a polonium deposit on a nickel plate which was inserted in the normal target position. The $B\rho$ value assumed for these particles was 3.3159×10^5 gauss-cm[13] which corresponds to an energy of 5.298 ±0.002 Mev. Since the magnetic fields were always measured in terms of the frequency of proton magnetic resonance, the spectrometer constants were calculated in terms of frequency. The spectrometer constant[21] for alpha-particles (C_α) was found to be $(1.0363\pm0.002)\times10^{-14}$ Mev-sec², and the constant for protons (C_p) was found to be $(1.0292\pm0.002)\times10^{-14}$ Mev-sec². Group energies calculated from these constants and from the magnetic resonance frequencies corresponding to the centers of the groups were corrected for energy loss in the target and for relativistic shift.

RESULTS

A spectrum obtained from the bombardment of a 0.14 mg/cm² foil target is shown in Fig. 1. Spectroscopic analysis showed that there was less than 0.1 percent of Na, Cu, and Fe in the target. Twenty inelastic proton groups were observed, nineteen appearing in this particular run. Two alpha-particle groups from the $Al^{27}(p,\alpha)Mg^{24}$ reaction corresponding to excitation of the 1.38-Mev and 4.14-Mev levels in Mg^{24} were found. These two are labelled "*c*" and "*i*"§ in the figure. Carbon deposits which formed during bombardment contributed another proton group which does not appear in Fig. 1 since these data were obtained immediately after a clean target was inserted. The proton group "*d*" was superimposed on the alpha-group "*c*" and was isolated by insertion of a 10 mg/cm² absorbing foil between the spectrometer exit-slit and scintillation detector.

The energy resolution obtained for these groups was about one percent. The width of the groups was attributed to several sources: (1) the proton beam had a half-width of 20 kev; (2) the angular acceptance of the spectrometer plus the angular divergence of the beam contributed 45 kev to the width of 6 Mev; (3) the finite resolution of the spectrometer ($\frac{1}{16}$-in. source and exit slit widths) contributed 31 kev to the width at 6 Mev.

The measured line shapes were quite good fits to a normal distribution function and exhibited little asymmetry. Application of Pearson's chi-square test to the data for five of the most intense inelastic groups resulted in an average probability of 0.5 for the normal dis-

TABLE I. Energy levels of aluminum.

Present work	Albarger and Hafner	Keller	Shoemaker *et al.*	VanPatter
0.844	0.84		0.82	0.86
1.016	1.02	0.97	1.045	1.02
	1.85			
2.259	2.15	2.39	2.225	2.12
2.782	2.78		2.75	2.72
3.046	3.04	3.17		
3.736	3.7			
4.018				
4.115				
4.473	4.3			
4.575				
4.647		4.71		
4.875				
4.996				
5.107				
5.220				
5.341	5.3			
5.501				
5.565				
5.620				
5.736	5.8	5.76		

[21] VanPatter, Sperduto, Huang, Strait, and Buechner, Phys. Rev. 81, 233 (1951).

§ *Note added in proof:* Subsequent investigations have shown peak "*i*" to be a doublet, corresponding to levels in Mg^{24} at 4.11 and 4.21 Mev.

tribution. Since a chi-square probability of 0.01 is considered satisfactory,[14] the lines were assumed to be normal in shape, and line centers were determined from the computed "best-fit" curves.

The energy levels determined for Al^{27} are shown in Table I and Fig. 2. The probable errors in these have been estimated as being 0.020 Mev from the uncertainty in determination of the group centers and from the uncertainty in the calibration constant. In Table I the levels listed by Alburger and Hafner,[15] which were the result of a literature survey covering the work reported before 1950, are given, along with more recent data reported by Keller,[5] by Van Patter, Sperduto, and Enge,[10] and by Shoemaker, Faulkner, Bouricius, Kaufmann, and Mooring.[16] It will be noted that in this experiment no scattering was observed corresponding to excitation of the 1.85-Mev level. Ten levels which were not previously reported were found.

We wish to acknowledge the help received from Dr. D. Halliday, Dr. L. Page, Dr. P. Stehle, from Mr. E. Perkins, Mr. R. Weise, Mr. J. Kane, as well as from the many other members of the Laboratory who have taken an interest in this project.

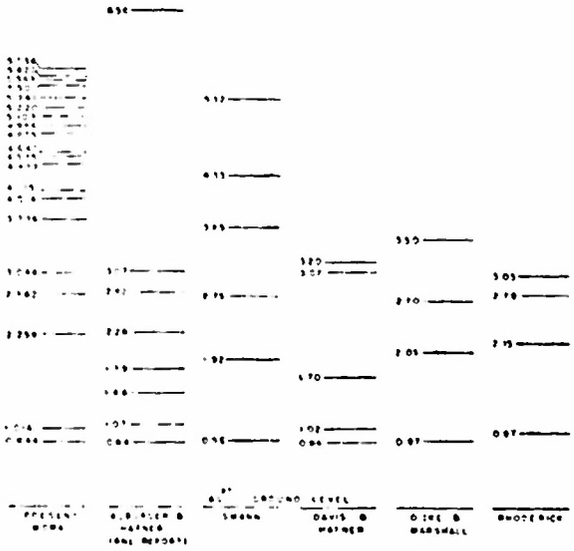

FIG. 2. Energy level scheme for Al^{27}.

[14] A. G. Worthing and J. Geffner, *Treatment of Experimental Data* (John Wiley & Sons, Inc., New York, 1946), pp. 183–184.

[15] D. E. Alburger and E. M. Hafner, Revs. Modern Phys. **22**, 373 (1950).

[16] Shoemaker, Faulkner, Bouricius, Kaufmann, and Mooring, Phys. Rev. **83**, 1011 (1951).

Reprinted from THE PHYSICAL REVIEW, Vol. 86, No. 6, 859-860, June 15, 1952
Printed in U. S. A.

Inelastic Scattering of Protons from Nickel*

RALPH ELY, JR.,† A. J. ALLEN, J. S. ARTHUR, R. S. BENDER, H. J. HAUSMAN, AND E. M. REILLEY‡
University of Pittsburgh, Pittsburgh 13, Pennsylvania

(Received February 18, 1952)

By use of the equipment developed for the precision scattering project at the University of Pittsburgh, inelastic scattering of 8 Mev protons from a thin nickel target has been observed at 90°. The energy levels obtained for natural nickel are 1.344, 1.479, 2.486, 2.526, 2.501, 2.660, 2.814, 2.946, 3.081, 3.161, 3.226, 3.308, 3.462, 3.575, 3.646, 3.773, 3.823, 3.944, 3.979, and 4.066 Mev. At present, only the three levels 1.344, 1.479, 2.501 Mev can be assigned to nickel 60 from comparison with beta decay of cobalt 60.

INTRODUCTION

ENERGY levels in nickel have been observed by the inelastic scattering of protons from a nickel foil. The apparatus and method of analysis of the data are the same as that of the preceding paper.[1] Dicke and Marshall,[2] with incident protons of 6.9 Mev, were unable to observe any levels in nickel. Fulbright and Bush,[3] using 5-17 Mev protons from the Princeton cyclotron, reported one weak level in nickel at 3.8 Mev as well as a broad band of tracks in the photographic emulsion used for detection. This broad band suggests either that a three-particle disintegration is occurring or that the levels are too close to be resolved with their equipment. In the present study, twenty energy levels have been observed.

The target (obtained from the Chromium Corporation of America) was a nickel foil of areal density 0.592 ± 2.5 percent mg cm^{-2}. Spectroscopic analysis showed less than 0.01 percent of copper in the target. The source and analyzer slits were $\frac{1}{8}$-inch wide. In all other respects the experimental details were essentially as reported in the preceding paper.

* Work done in the Sarah Mellon Scaife Radiation Laboratory and assisted by the joint program of the ONR and AEC and the Research Corporation.

† Now at Westinghouse Atomic Power Division, Bettis Field, Pittsburgh, Pennsylvania.

‡ Now at Camp Evans Signal Laboratories, Belmar, New Jersey.

[1] Reilley, Allen, Arthur, Bender, Ely, and Hausman, Phys. Rev. **86**, 857 (1952).

[2] R. H. Dicke and J. Marshall, Phys. Rev. **63**, 86 (1943).

[3] H. W. Fulbright and R. R. Bush, Phys. Rev. **74**, 1323 (1948).

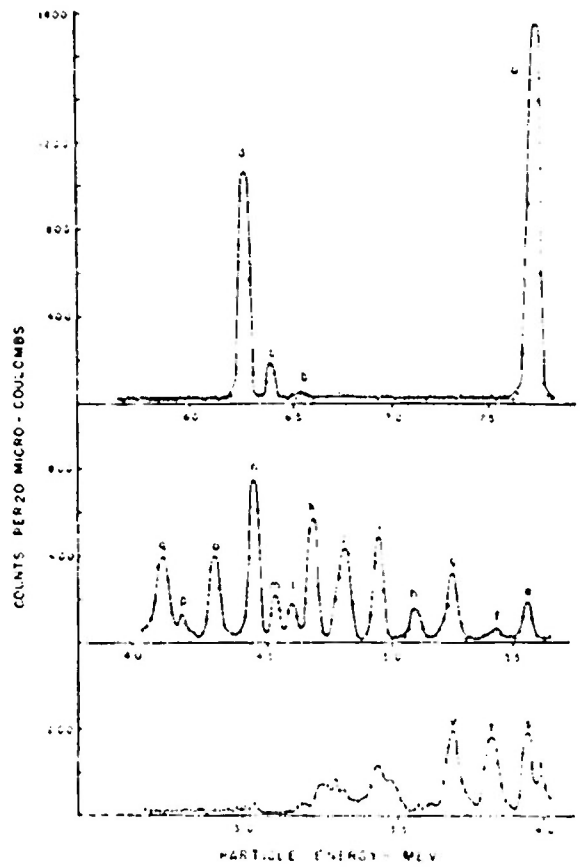

FIG. 1. Spectrum of protons scattered from nickel at 90°.

RESULTS

Figure 1 shows the energy spectrum obtained for 8-Mev protons scattered from nickel at 90°. Inserting absorption foils in front of the detector shows that all are proton peaks. Peak "*a*" is the nickel elastic peak, while "*b*" is the elastic peak caused by a thin carbon deposit which formed during bombardment. Table I shows the energies of the resultant levels; they are corrected for recoil nucleus, relativistic, and target energy loss effects. A probable error of the order of 20 kev seems reasonable. Below 3.6 Mev in Fig. 1 are several partially resolved peaks. Tentative but questionable assignment of these peaks are: 4.29, 4.33, 4.44, 4.47, and 4.50 Mev.

Figure 2 shows the energy level scheme for nickel. Brady and Deutsch,[4] from beta-decay of Co^{61}, report

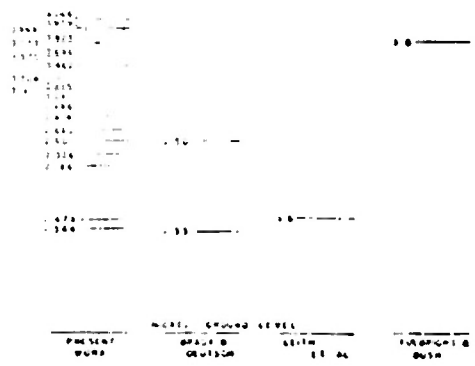

FIG. 2. Energy level scheme for nickel.

TABLE I. Energy levels of nickel.

Level	Energy Mev	Brady and Deutsch Mev	Leith *et al.* Mev	Fulbright and Bush Mev
c	1.344	1.33		
d	1.479		1.5	
e	2.186			
f	2.326			
g	2.501	2.50		
h	2.660			
i	2.814			
j	2.946			
k	3.081			
l	3.161			
m	3.226			
n	3.308			
o	3.462			
p	3.575			
q	3.646			
r	3.773			
s	3.823			3.8
t	3.944			
u	3.979			
v	4.066			

levels of 1.33 Mev and 2.50 Mev in Ni^{60}. The third level is at 1.5 Mev in Ni^{63} as reported by Leith, Bratenahl, and Moyer[5] from positron decay of Cu^{60}. The remaining levels are as yet unassigned to a particular isotope. The level obtained by Fulbright and Bush[3] is shown at 3.8 Mev.

We wish to acknowledge the help received from Dr. D. Halliday, Dr. L. Page, Dr. P. Stehle, Mr. E. Perkins, Mr. R. Weise, and Mr. J. Kane, as well as from the many other members of the Laboratory who have taken an interest in this project.

[4] E. L. Brady and M. Deutsch, Phys. Rev. **74**, 154 (1948).
[5] Leith, Bratenahl, and Moyer, Phys. Rev. **72**, 732 (1947).

Reprinted from THE REVIEW OF SCIENTIFIC INSTRUMENTS, Vol. 23, No. 10, 572-573, October, 1952
Printed in U. S. A.

Radiofrequency Power Supply*

L. M. REILLY, † R. S. BENDER, AND H. L. HAUSMAN
Radiation Laboratory, University of Pittsburgh, Pittsburgh, Pennsylvania
(Received November 9, 1951)

A HIGH voltage power supply has been designed having a maximum current output of 500 microamperes for use with any equipment wherein very high dc stability of the supply voltage is essential. The input to the regulation section of the supply is a dc amplifier wired as a difference amplifier, the dc reference voltage supplied by a 5651 voltage regulator tube operating at constant current. Because of the two stages of dc amplification, the plate swing of tube V3 is limited to ±50 volts. It is desirable that the plate of V3 be at about 225 volts, the mid point of its range, under actual load conditions. The screen bias of V5 may be set in two ways. Either the plate of V3 may be connected directly to the grid of V2B and an OA2 or OB2 VR tube used to obtain proper screen bias, or a high resistance chain (R_1,R_2) may be used to drop part of the voltage applied to the grid of V2B. The following procedure may be used to tune the plate circuit of the oscillator. A variable condenser, 400-1000 $\mu\mu$f, is placed in the tank circuit of the 6AQ5 oscillator. Under load conditions—external load at desired potential—the condenser is tuned to minimize the screen potential of V5.

An output voltage from 500 to 3000 volts is obtained by use of the wire wound resistance chain. The switch gives 500-volt steps and the 100K potentiometer a continuous control over the range. A 2K precision resistor is included in the fixed chain for measuring the absolute value of the output voltage with a potentiometer.

The dc output voltage measured over a period of 48 hours shifted less than two parts in 10,000; over a period of ½ hour, the deviation was less than one part in 10,000. For these determinations, a well regulated 300-volt supply was used. The ac ripple content in the output dc has been measured as being less than 10 millivolts.

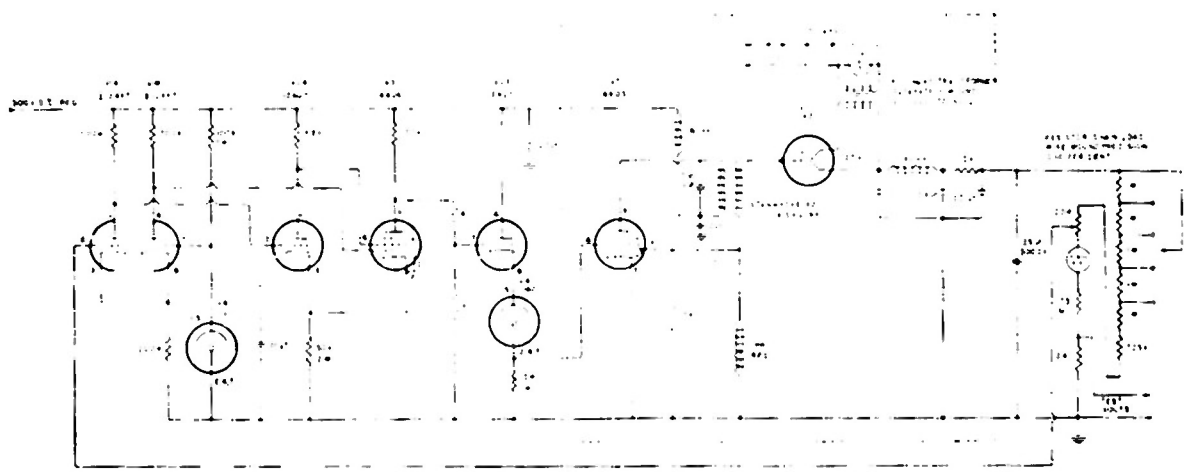

FIG. 1. High voltage power supply.

Dr. B. L. Robinson of The Johns Hopkins University has tried a simple method for conversion of the present supply to a negative output. The technique is to ground the B + of the 300-volt supply for the regulation section. In order to get a suitable grid reference voltage it is necessary to use 5651 tubes in series from ground to the grid of V1B.

* Work done in the Sarah Mellon Scaife Radiation Laboratory and assisted by the joint program of the ONR and the AEC.
† Now at Camp Evans Signal Laboratories, Belmar, New Jersey.

Reprinted from THE REVIEW OF SCIENTIFIC INSTRUMENTS, Vol. 23, No. 10, 542–547, October, 1952
Printed in U. S. A.

The University of Pittsburgh Scattering Project*

K. S. BENDER, E. M. REILLEY,† A. J. ALLEN, R. ELY,‡ J. S. ARTHUR, AND H. J. HAUSMAN
Radiation Laboratory, University of Pittsburgh, Pittsburgh, Pennsylvania

(Received January 5, 1952)

A scattering program at the University of Pittsburgh uses charged particles from the cyclotron (8-Mev protons, 16-Mev deuterons, and 32 mev alpha-particles). An electromagnet focuses the cyclotron beam through an aperture in an 8-ft shielding wall into a scattering laboratory; a second magnet analyzes the beam in energy; a third magnet analyzes the energy of the charged particles produced in the reaction. For $\frac{1}{16}$-in. analyzing slits 1.0 microamperes of 8±0.010-Mev protons are available at the target 31 ft distant from the cyclotron. The reaction particle analyzer can be rotated about the target. The energy dispersion for 5.298-Mev alpha-particles is 0.192 Mev in. for each analyzer; the momentum resolution is 1 part in 850. The detector is a scintillation counter. The energy determinations at present stage of development are thought to be accurate to ±0.2 percent ascribed to magnet calibration uncertainties. Energies above and below this value are thought to be of the same precision but the actual calibrations have not been completed.

INTRODUCTION

THE University of Pittsburgh cyclotron accelerates protons to an energy of 8 Mev, denterons to 16 Mev, and alpha-particles to 32 Mev. Radiation background makes the direct study of nuclear reactions in the cyclotron chamber itself very difficult. Also the spreads in angle and in energy of the cyclotron external beam are large and attempts to reduce these factors by simple collimation would greatly reduce the beam intensity. To overcome these obstacles a shielded scattering laboratory was built into a hillside just behind the cyclotron chamber. An 8-ft wall was placed between these two rooms. One can work safely in the scattering laboratory with the cyclotron operating as long as the beam is not focused into the room. An aluminum duct system transports the incident beam 31 feet through focusing and beam analyzing magnets to the scattering chamber; the charged particles from the reaction traverse an additional 10 feet of duct system through a second analyzing magnet to a scintillation detector. For 8-Mev protons a normal beam at the target through $\frac{1}{16}$-in. slits is 1.0 microampere with an energy spread of ±0.010 Mev.

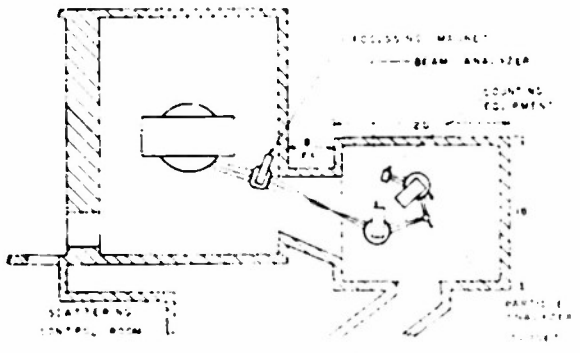

FIG. 1. Plan view of the cyclotron and the scattering project.

BEAM FOCUSING AND ANALYSIS

An electromagnet in the cyclotron room (see Fig. 1) is designed to focus the cyclotron beam on to an adjustable slit located in the 18-in. high water tank which forms part of the shielding wall. Since the cyclotron beam has no well-defined source, a single magnet cannot well be used for focusing and for precise energy analysis of the beam. By using separate focusing and analyzing magnets, it is possible to remove this limitation. At the same time the focusing magnet increases the distance between the cyclotron and target and enables better shielding of the counting area from the cyclotron background radiation.

A slit located at the focal point of the focusing magnet, serves as an effective source for the beam analyzing magnet. The slit is 1 in. high and formed from 2 pieces of $\frac{1}{8}$-in. thick tantalum with carefully machined edges. From a position in the scattering laboratory (without breaking the vacuum) its width may be adjusted to within ±1 mil. Modified Helmholtz coils along the duct in front of the focusing magnet are used to raise and lower the cyclotron beam.

The second magnet is used for energy analysis. It is placed in the scattering laboratory close to the shielding wall and produces an image of the adjustable slit at a point near the center of the room. This magnet was calibrated by using alpha-particles from polonium. The magnetic field strength in the gap was measured by a proton magnetic resonance detector. The $H\rho$ value used for the polonium alpha-particles was 3.3159 $\pm 0.0007 \times 10^6$ gauss-cm as reported by Van Patter *et al*[1]; this corresponds to an energy of 5.298±0.002 Mev.

Two sets of adjustable stops are used to define the beam in angular spread. The first is placed in front of the pole tips of the focusing magnet and allows a maximum total spread of 10 degrees. The second is placed in front of the pole tips of the beam analyzing magnet, allowing a maximum total beam spread of 8 degrees.

* Work done in Sarah Mellon Scaife Radiation Laboratory and assisted by the Joint Program of the ONR and the AEC, and the Research Corporation.

† Now at Camp Evans Signal Labs, Belmar, New Jersey.

‡ Now at Westinghouse Atomic Power Division, Bettis Field, Pittsburgh, Pennsylvania.

[1] Van Patter, Sperduto, Huang, Straight, and Buechner, Phys. Rev. 81, 233 (1951).

To facilitate tuning the cyclotron, insulated drop probes or beam catching plates connected to remote microammeters are located at (1) the cyclotron exit port (a drop probe), (2) just in front of the focusing magnet (top and bottom plates), (3) behind the focusing magnet (a drop probe), (4) at the adjustable slit (top, bottom, right, and left plates), and (5) in the scattering chamber (top and bottom plates).

A brass plate with a milled slit $\frac{1}{16}$ in.$\times$1 in. is located at the focal point of the beam analyzer. The target is placed $1\frac{3}{4}$ in. beyond this slit. Since the targets used are very thin foils most of the beam passes through and is collected in a Faraday cup placed eight inches from the target. This cup is connected by means of a polyethylene insulated coaxial cable to either a current integrator or a microammeter. Beam currents of 1.0 microamperes for continuous operation can be obtained. Under these conditions the cyclotron beam current to the drop probe at the cyclotron exit port is 120 microamperes and that to the probe behind the focusing magnet is 40 microamperes.

REACTION PARTICLE ANALYSIS

A third magnet was constructed to measure the energies of the charged particles emitted from the target. It is mounted on a rotatable carriage; a sylphon coupling is arranged between the scattering chamber exit ports and the reaction analyzer vacuum duct system so that studies can be made at a continuous range of scattering angles up to within 30 degrees of the normal center line of the incident beam. A set of adjustable stops defines the total angular spread of the emerging particles up to a maximum of 10 degrees.

SCATTERING CHAMBER DESIGN

A plan view of the scattering chamber is shown in Fig. 2. This chamber was formed of $\frac{3}{4}$-in. aluminum (alloy 61-ST) by rolling from a 6-in. wide strip. After rolling into a ring of $14\frac{1}{2}$-in. i.d., the joint was arc-welded in an argon atmosphere. Machining of gasket groves and ports was done after this welding operation. Top and bottom plates of $\frac{3}{4}$-in. aluminum (alloy 61-ST) were pinned in position by one small blind steel pin each.

The target holder is mounted on the top of a brass tube which is located on the axis of the scattering chamber. The target foils are mounted between two small rectangular frames which are bolted together thus clamping the foil along its four edges. Three of these foil mounts can be placed in the target holder at one time, one above the other. An O-ring seal around the brass supporting tube permits any one of the three to be placed in the beam without disturbing the vacuum. Provision is also made for heating the targets in place to minimize the formation of carbon deposits on the targets. A Faraday cup is placed in the zero degree port and intercepts the beam passing through the target. A $\frac{1}{2}$-in. long cylindrical insulated guard ring is placed in front of the Faraday cup.

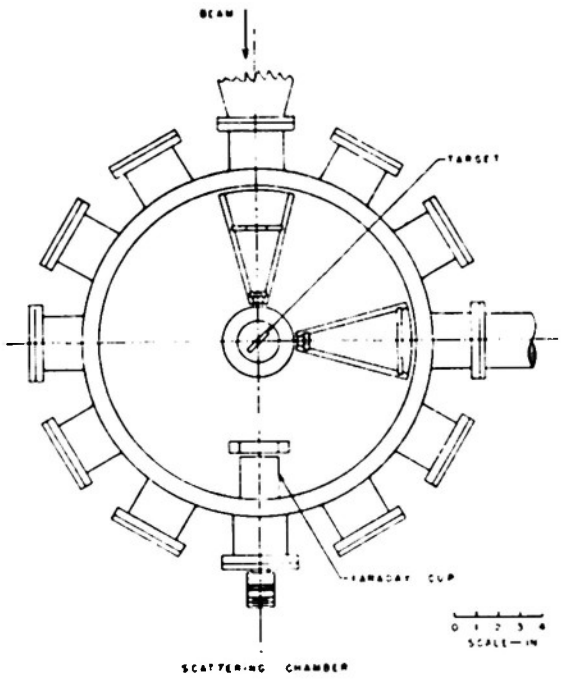

FIG. 2. Plan view of the scattering chamber.

The slit which defines the energy spread of the beam incident on the target is rigidly attached to the scattering chamber; the slit system defining the angular spread of the emergent particle beam can be pivoted horizontally about the center of the chamber. The solid angle intercepted by the particle analyzing magnet is determined by a single slit located in this emergent particle slit system.

MAGNET DESIGN

The three magnets were designed to produce fields large enough to focus 16-Mev deuterons or 32-Mev alpha-particles. The $H\rho$ value for either of these two particles is 810 k-gauss-cm. If one chooses a nominal value of 13,000 gauss for the magnetic field, the radius of curvature is 62.5 cm. The energy dispersion for 8-Mev protons is 0.320 Mev/inch. An energy spread of $\pm$0.010 Mev for 8-Mev protons is thus obtained with $\frac{1}{16}$-in. analyzing slits.

Design of the magnet was conservative in anticipation of possible increased cyclotron beam energy. As a result, the magnetic fields of the completed magnets are relatively linear with current up to 16,000 gauss and a field of 18,000 gauss can easily be achieved.

Mainly for shielding reasons the target position was chosen to be about 31 feet from the cyclotron exit port. The architecture then dictated that the straight line distance between source and image be 190 in. for the focusing magnet and 155 in. for the beam analyzer. The resultant deflection angles are 14 degrees for the median ray through the focusing magnet and 40 degrees for the median ray through the beam analyzer. The straight line distance between source and image for the

reaction particle analyzer was chosen to be 82 in., if it were larger the magnet could not be rotated about the target in the scattering room. Its median ray is deflected through 60 degrees. The magnets were designed to accommodate the normal 10-degree total angular spread of the cyclotron beam.

The magnet yokes are C type, with rectangular cross section, flame cut from the appropriate thickness of annealed SAE 10-20 steel. The faces of the C yokes were machined parallel to ±2 mils. Seven-inch pole pieces, coil cores, are bolted to these machined faces. To these pole pieces are bolted 1-inch thick iron slugs having a shape and size intermediate between that of the pole pieces and that of the sector shaped pole tips which are also 1-in. thick. These intermediate slugs are made with rounded corners in order that vacuum seals may be made to them. The magnet air gaps were chosen as 1 in., which is a compromise between the thickness of the emergent cyclotron beam and the power requirements of the magnets.

The focusing magnet consists of 2664 turns, with 5 tons of iron and 667 pounds of copper. The beam analyzing magnet and reaction particle analyzing magnet have 3848 turns with 6 tons of iron and 964 pounds of copper. These two analyzing magnets are similar except for the shape of the intermediate slugs and pole tips.

The coils are wound with copper strap $\frac{1}{4}$ in. wide by 60 mils thick which includes a 10-mil thickness of silicone-varnish impregnated glass insulation. Sub-coils are first wound to produce a coil $\frac{1}{4}$-in. wide and 75 turns deep. Pairs of these sub-coils are assembled side by side such that their windings are in opposite directions. The inner turns are soldered together. The coil-pairs are then sandwiched between $\frac{1}{16}$-in. thick copper disks and the outer turns of adjacent coil-pairs are soldered together. Water cooling is accomplished by soldering copper tubing to the outer rims of the copper disks.

TRIMMING OF THE POLE TIPS

Two problems arise in the positioning of the pole tips relative to the magnet slugs and yoke. First, repositioning the tips on the intermediate slugs, and second, obtaining a constant reproducible gap width. The positioning relative to the intermediate slugs was accomplished by dowel pinning the tips to the slugs at two points.

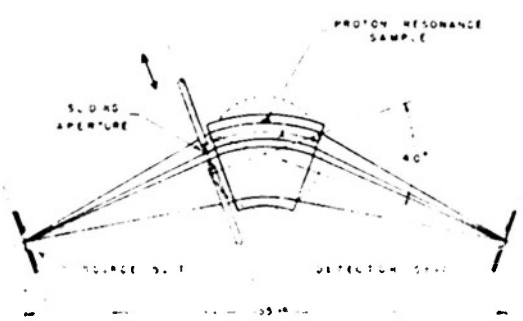

FIG. 3. Magnet trimming arrangement. Plan view of a pole-tip of the beam analyzing magnet showing the source and detector slits and the sliding aperture.

In order to insure a constant, reproducible gap width, the jaws of the yoke were jacked apart and stainless steel permanent spacers were inserted between the intermediate slugs at 4 points. Four inclined plane jacks were placed in each air gap to hold the pole tips against the intermediate slugs. The air gaps are reproducible to within 5 parts in 10^4.

In designing the three magnets account was taken of first-order deviations from optimum focus due to the fringing field of the sectors. The method is an extension of the work done by Coggeshall[2] and by Roters.[3] Second order deviations were corrected empirically by ascertaining the magnetic field necessary for focusing monoenergetic particles through various arc segments of the air gap and removing iron from the tips where necessary. The empirical cutting procedure for the beam analyzing magnet and the reaction particle analyzing magnet are similar, and hence, only the procedure for the beam analyzing magnet will be discussed.

Two slits ($\frac{1}{16}$ in. wide and 1 in. high) were placed at the approximate source and image position of the magnet. A polonium alpha-source was placed in front of the input slit. Behind the detector slit was placed an RCA-5819 photomultiplier tube with a scintillation screen of zinc sulfide mounted on a Lucite light pipe. All of the magnet gap was blocked to the passage of alpha-particles except for a $\frac{1}{2}$-in. window which could be moved laterally across the magnet gap in $\frac{1}{2}$-in. steps. (see Fig. 3). At each step the counting rate was determined as a function of the magnetic field. From these data one can determine the magnetic field value, expressed in terms of the proton resonance frequency, which is necessary to focus the monoenergetic polonium alpha-particles at each $\frac{1}{2}$-in. step. Such a curve is shown in Fig. 4 marked "f_{max} original." An arbitrary frequency f_0, which was higher than any of the observed frequencies, was chosen (in this example $f_0 = 21.700$ mc/sec). As a first approximation for determining the amount of material to be removed at each point along the pole tips, the expression $\Delta l/l = (f_0 - f_{max})/f_0$ was used, where Δl is the material to be removed and l is the particle path length in the magnetic field. This method of calculating the amount of material to be removed from the edges of the pole tips is conservative. After the first few cuts, however, a correlation appeared between the amount of material removed from a definite position and the improvement in focusing at the same point. This empirical correlation is used to guide the subsequent cuts. Cutting was stopped when the maximum deviation in relative focusing of the monoenergetic alpha-particles at the various segment positions fell within the error caused by failure to reproduce the gap width. After the final cut, the maximum deviation

[2] N. D. Coggeshall, J. Appl. Phys. 18, 855 (1947).
[3] H. C. Roters, *Electromagnetic Devices* (John Wiley & Sons Inc., New York, 1941).

from the mean of the proton resonance frequency for focusing at each point was less than 3 parts in 10,000.

To determine the dispersive power of the magnet, the target slit was replaced by two $\frac{1}{16}$-in. slits separated $\frac{1}{4}$ in. in the image plane. A curve of particle count *versus* magnetic field with full magnet aperture gave a value for the dispersive power, for 5.298-Mev alpha-particles, of 0.192 Mev/in. Line shapes using the polonium source were taken with full aperture to determine the resolving power of the magnets. A value of the order of one part in 850 of momentum was found after corrections had been made for source thickness.

The beam focusing magnet in the cyclotron room was also trimmed empirically. The cyclotron beam was used as a source while a Faraday cup behind the adjustable slit was used as a beam collector. The beam intensity was measured with a galvanometer. The data for final trimming were obtained using the beam analyzing magnet set to focus cyclotron protons at approximately the median energy of the cyclotron spectrum. The criterion for cutting was then dictated by the condition that the maximum number of particles of the selected energy range be focused into the scattering chamber.

After the magnets had been trimmed and positioned for a scattering experiment, repeated calibration checks were made. If air had not been admitted to the system between calibration runs, the probable error in reproducing the calibration constant was 4 parts in 10^4. However, over a 4-month period, the system was down to air many times for checks and adjustments. The probable error in reproducing the calibration constant over this period rose to 4 parts in 10^3. It is believed that this failure to reproduce the calibration constant is due to small geometrical shifts in the system when the system is being either pumped down to vacuum or opened to air. To correct for these uncertainties, it is planned to place a remotely controlled polonium line source at the adjustable slit and one at the target holder permitting a check on the calibration constants at any time during the experiment.

DETECTION AND COUNTING ARRANGEMENT

The detector adopted is a scintillation screen and photomultiplier tube mounted outside the vacuum system. A 0.05-mil nickel foil is cemented to the back of the detector slit as a vacuum seal. The photomultiplier tube (EMI type 5311) is encased in an aluminum tubing light shield such that it can be adjusted in position axially and brought as close as is practical to the nickel window. A zinc sulfide screen is deposited on a piece of a glass lantern slide ($\frac{1}{2}$ in.×1 in.) by settling from an alcohol-water suspension. This screen is taped to the photosurface part of the tube with Scotch cellophane tape. A small amount of microscope immersion oil is placed between the tube face and the glass plate so that good optical contact is obtained.

Zinc sulfide was chosen for the scintillation screen for several reasons. The efficiency of a thin ZnS screen

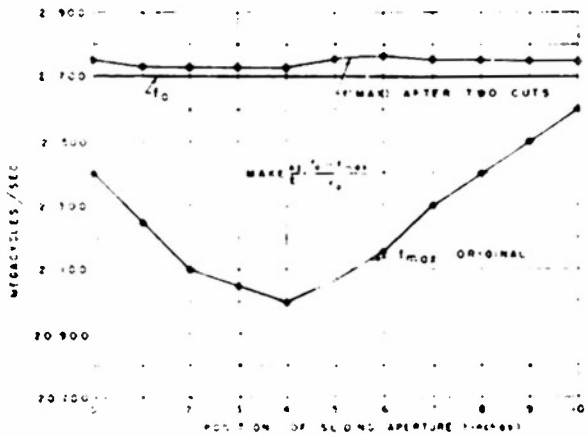

FIG. 4. Plot of the magnetic field necessary to focus Po alpha-particles at $\frac{1}{4}$-in. openings along the pole-tip edge. The bottom curve was taken prior to trimming. The top curve represents the second of a series of cuts.

for gamma-ray and neutron background radiation is small as compared to other crystals checked. It was also found that for an appropriate thickness of ZnS, the pulse-height distribution for charged particles is approximately independent of energy over a wide range. Thus, it is not necessary to continually change the bias settings of the input discriminators to the scaling circuits as particles of different energies are counted.

By using an EMI 5311 photomultiplier tube, and with polonium alpha-particles incident on a ZnS screen, forty-volt pulses of narrow half-width are obtainable with a good signal to noise ratio. The pulses from the photomultiplier collector are fed into a cathode follower consisting of a parallel connected double triode (12 BH7), which is necessary to drive the eighty-foot length of RG7 U coaxial cable that conducts the pulses to the counting system. This cable is terminated with a 100-ohm resistor in order to minimize reflections. The terminated cable is connected to the input of a Jordan and Bell linear amplifier[4] modified to have a faster rise-time at the expense of gain. Output pulses from this amplifier are inserted into the input discriminator of a scaling circuit. This consists of one Model 108 and one Model 109 decade counting strip§ and a Veeder Root mechanical register.

A remotely controlled swinging gate is included in the vacuum system of the reaction particle magnet so that all particles from the scattering chamber can be intercepted. This is helpful in determining the countable background due to gamma-ray and neutron fluxes in the scattering laboratory. Also included is a remotely controlled polonium alpha-particle source which can be swung in front of the detector slit. This is convenient for adjusting the photomultiplier tube voltage and the amplifier gain, and enables counting conditions to be

[4] W. H. Jordan and P. R. Bell, Rev. Sci. Instr. **18**, 703 (1947).
§ Atomic Instrument Company, Boston, Massachusetts.

reproduced from day to day. It is also of some value in identifying the types of particles being counted.

Identification of reaction products—in general, alpha-particles and protons—is made by means of aluminum foils. Since protons and alpha-particles of the same energy are focused by the same magnetic field, differentiation is accomplished by using the difference in specific ionization of the two particles. For a certain thickness of absorber, alpha-particles will be stopped while protons of the same initial energy will pass through at reduced energy. A remotely controlled foil injector system is mounted directly preceding the detector slit in the duct system of the particle analyzing magnet. In addition to the foils used for distinguishing proton and alpha-particles, a second set of foils is used to decrease the energy of the particles from a fixed energy proton resonance level—in general, the elastic scattering peak—in known energy decrements. This process gives a rough measurement of the efficiency of the scintillating material as a function of energy.

In an attempt to reduce background radiation resulting when the beam of 8-Mev protons strikes the angular collimators, target slits, and Faraday cup, various high atomic number materials were tested to determine their activities relative to the present collimating materials—namely, brass and aluminum. The activities for tantalum and tungsten were approximately $\frac{1}{4}$ the activity of brass for the same number of incident particles; the activity for molybdenum was $\frac{1}{2}$ that for brass. It is planned to cover all areas exposed to the beam in the scattering laboratory with tantalum.

Integration of the beam current is accomplished by connecting the Faraday cup to a pre-charged condenser and observing the discharge with a quartz fiber quadrant electrometer made by the Cambridge Instrument Company. A bank of polystyrene-insulated condensers with a capacity of one microfarad and charged to a potential of 10 volts is used. The electrometer is used as a null indicator. With a typical beam current of 0.5 microampere collected by the Faraday cup a counting interval consists of a twenty-second period in which 10 microcoulombs of charge are transferred. The relative accuracy in beam current integration under these conditions is of the order of one part in 500. An automatically operating electronic current integrator has just been developed to replace the manually operated integrator.

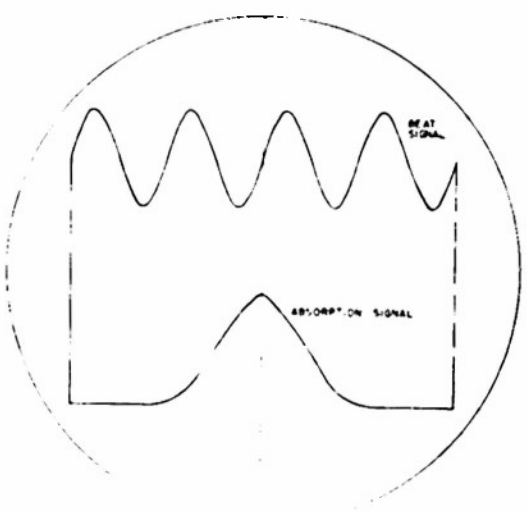

FIG. 5. Oscilloscope pattern showing the proton absorption signal on the lower trace and on the upper trace, the beat signal between a frequency meter and the magnetic resonance oscillator frequency.

MAGNETIC FIELD MEASUREMENTS

Magnetic field measurements are made by measuring at resonance the frequency f of a proton magnetic resonance oscillator whose absorption signal width at half-maximum is 0.5 gauss. This frequency is related to the magnetic field B by

$$B=2\pi f/\gamma, \tag{1}$$

where γ is the nuclear gyromagnetic ratio.

The radiofrequency oscillator is somewhat similar to that used by Pound and Knight.[5] The audiofrequency component of the oscillator output is detected by a diode rectifier, amplified by a high gain audio-amplifier, and fed to a coaxial cable. In the control room the signal from the cable is further amplified and injected into an electronic switch.

In the same chassis with the oscillator is an anode follower which feeds a small portion of the radiofrequency output of the oscillator through another coaxial cable to a frequency meter in the control room. It also serves to isolate the proton absorption signal channel from the audio beat note of the frequency meter.

The electronic switch drives an oscilloscope which displays two traces simultaneously (see Fig. 5). The top trace displays the beat frequency output of the frequency meter while the bottom trace displays the absorption signal.

DATA TAKING AND PERFORMANCE

The chain of operations followed in order to obtain an accurately known magnetic field is as follows. The frequency meter is tuned to an appropriate subharmonic of the frequency f given by the relationship (Eq. 1). The remote selsyn dial connected to the tuning condenser of the magnetic resonance oscillator is tuned until a zero beat frequency appears on the top trace of the oscilloscope pattern. Finally, the magnetic field is varied by changing the magnet current until the absorption signal appears on the lower trace. By using the zero beat displayed, frequencies can be measured to within 1 part in 50,000; the magnetic field can be set, using the center of the absorption peak, to within $+0.1$ gauss.

[5] R. V. Pound and W. D. Knight, Rev. Sci. Instr. 21, 219 (1950).

All magnetic fields are held constant to better than 1 part in 50,000 by electronic current regulators. Essentially the operation consists of a comparison, by means of a Brown vibrator, of an adjustable potential with a sample voltage taken from a manganin resistor in the magnet circuit. The difference is amplified and phase detected for use in controlling the field excitation of a 500-watt amplidyne which in turn supplies the excitation for a 5-kw generator supplying the magnet current.

The energy increments used in surveying the energy levels of a particular nucleus are determined primarily by the energy spread of the incident beam. In general with $\frac{1}{16}$-in. slits for the energy analyzing magnet which defines the energy as 8±0.010 Mev, the magnetic field of the reaction particle magnet is changed in 0.010-Mev steps. The time necessary for a survey run may amount to 36 hours of continuous running. Throughout the run, the magnetic field of the beam analyzing magnet remains fixed to within ±0.1 gauss. Over the total running period only minor adjustments need be made on the tuning of the cyclotron permitting continuous currents of the order of 1.0 microamperes to be maintained with a total variation in beam intensity of ±10 percent.

To date the energy levels of Al, Ni, Au, Bi, Cu, C have been surveyed. Nickel and copper targets have been generously supplied by the Chromium Corporation of America, Waterbury, Connecticut. A typical survey run is shown in Fig. 6. A thin target (0.63 micron) of naturally occurring copper was bombarded with 8-Mev protons having an energy spread of ±0.010 Mev and the reaction products observed at 90 degrees to the incident beam. The angular spread of the incident beam was ±3 degrees; of the outgoing beam, ±2 degrees. Peaks *a*, *b*, and *d* of the Cu spectrum are the elastic peaks of copper, oxygen, and carbon, respectively. However, the overlap seen on peak *d* is probably due to a superposition of the 0.96-Mev energy level of Cu^{63} and the carbon elastic peak. Peaks *i* and *r* have been tentatively assigned to the 1.89-Mev level and the 2.60-Mev level of Cu^{65}, respectively. A tentative assignment of peak *e* to the 1.12-Mev level of Cu^{65} and peak *g* to the 1.49-Mev level of Cu^{63} can also be made.

Except for peaks *c* and *t* of the Cu spectrum, it can be seen that peaks *a* through *z* are resolved sufficiently so that energy levels could be assigned. However, most of the proton peaks of energy less than 4.0 Mev are not sufficiently resolved by our apparatus at present to permit an accurate assignment of levels. The complexity of the spectra from nuclei with mass number near Cu is approaching the limit of resolution of our apparatus. For the copper run, counting intervals were averaging a minute per experimental point using $\frac{1}{16}$-in. detector and source slits and having beam currents on the order of 0.7 microampere.

It is believed that a significant increase in the peak-to-background intensity ratio can be obtained by using tantalam as a beam stopping material in the counting laboratory to reduce background radiation. Also, the resolution of the system can be increased by decreasing the angular and energy spreads of the incident beam. This would mean longer running times due to the decrease in beam intensity.

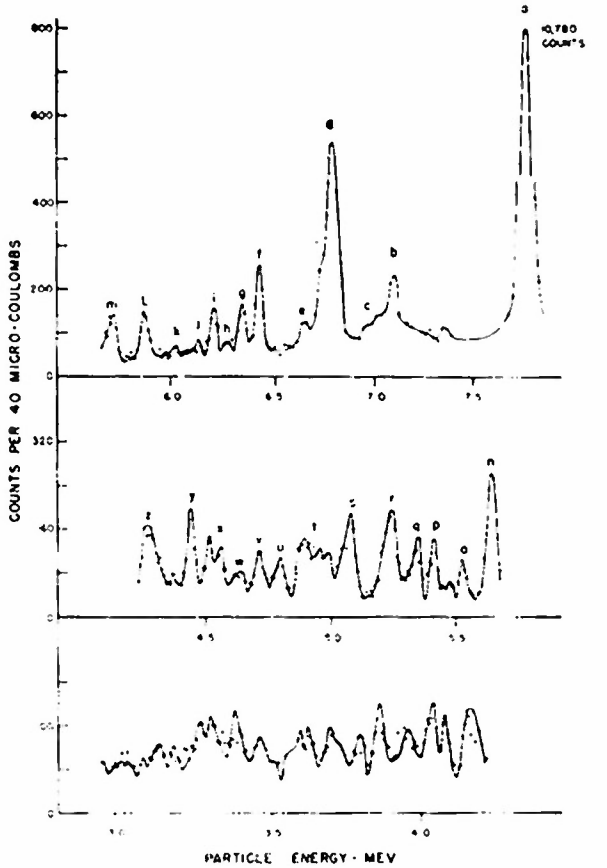

FIG. 6. Spectra of charged particles emitted from copper at 90°. A plot of the counts per 40 micro coulombs of 8-Mev protons through the target *versus* scattered particle energy.

CONCLUSION

The scattering apparatus represents a flexible experimental tool for extending nuclear measurements of Van de Graaf precision to the region of medium energies. With this equipment experiments can be performed under clean observational conditions of low background, precise control of energy and energy spread, and good collimation. Angular correlation studies are planned.

The authors wish to thank Dr. David Halliday, Dr. Lorne A. Page, and Mr. Clayton J. McDole, who helped in the early stages of development. They are also indebted to Mr. Robert F. Weise, Mr. John F. Kane, and Mr. Eugene M. Perkins for their help in the design and development stages of the project.

Reprinted from THE PHYSICAL REVIEW, Vol. 88, No. 2, 424, October 15, 1952
Printed in U. S. A.

The Quenching of *Ortho*-Positronium Decay by a Magnetic Field*

JOHN WHEATLEY† AND DAVID HALLIDAY
University of Pittsburgh, Pittsburgh, Pennsylvania
(Received September 3, 1952)

WE have measured the quenching of three-quantum annihilation from positronium by a magnetic field.[1] This effect has been detected by Deutsch and Dulit[2] and by Pond and Dicke[3] using different methods. Positronium was formed in SF_6 gas in a chamber placed between the poles of a magnet. The positron source was ~0.01 mc Na^{22} on a Zapon film. The decay of the $^3S_1$ positronium was detected by three NaI scintillation counters placed with their axes 120° apart in the plane perpendicular to the magnetic field.[4] The background triple coincidence rate was found by letting nitric oxide into the gas chamber. Generally, the background was about ten percent of the total triple coincidence rate. The magnet was specially designed and the 5819 photomultipliers magnetically shielded to eliminate magnetic field effects on the counters. At a given pressure we measured the ratio $n(H)$ of the true triple coincidence rate at the field H to that at $H=0$.

If one plots $n(H)$ against $(1-n)/H^2$, one should obtain at low enough gas densities a straight line whose intercept is the fraction of the rate contributed by the $^3S_1$, $m_J=\pm1$ states. A typical experimental curve is shown in Fig. 1 for a density of 0.052 g/cm³. It is clear that the $m_J=\pm1$ states supply less than two-thirds of the zero field rate. This is in agreement with calculations by Drisko[5] who finds that the probability for annihilation from any particular m_J substate of the $^3S_1$ state depends on the angle of the plane of the annihilation with the external field. In the special case corresponding to our geometry, Drisko finds that the $m_J=0$ state contributes one-half of the zero field rate. All our data are in agreement with this result.

If collisions are ignored, the theoretical expression for $n(H)$ for our geometry is

$$n(H)=(2+a^2r_0)/(2+2a^2r_0),$$

where $r_0=\tau_3/\tau_1=1120$ as given theoretically by Ore and Powell,[6] and $a=2\mu_0H/\Delta E$ with ΔE the ground state splitting as determined recently by Deutsch and Brown.[7] If one includes the possibility that collisions with gas atoms can cause transitions from $J=1$ to $J=0$ (probability per unit time $\lambda=N v\sigma$) and transitions in which m_J changes with $\Delta J=0$ (probability per unit time $\lambda'=N v\sigma'$),

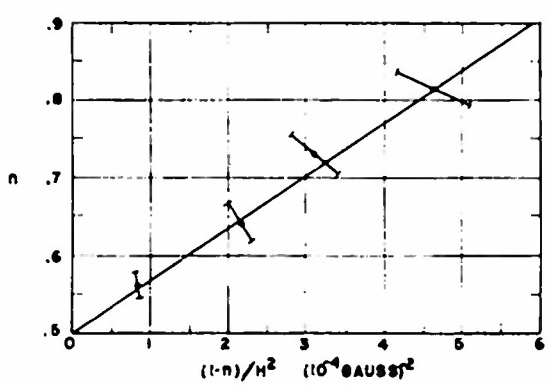

FIG. 1. A quenching plot for an SF_6 density of 0.052 g/cm³.

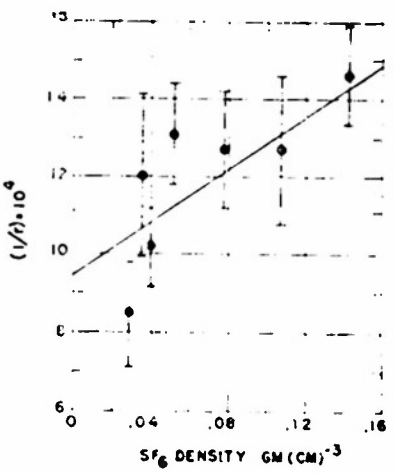

FIG. 2. A least squares line whose intercept gives r_0 and whose slope gives σ.

the situation is more complicated.[8] Transitions of the latter type cause $n(H)$ to approach a high field limit of less than $\frac{1}{2}$.

At high fields the quenching is relatively more sensitive to λ' than to λ. We found by measuring $n(H)$ as a function of gas density at $H=7100$ gauss that $\sigma'<\frac{1}{3}\sigma$. This conclusion depends on making use of a value of σ reported by Siegel and De Benedetti[9] for SF_6 ($\sigma\approx10^{-21}$ cm²). Using this approximate limit for σ', we find that for $H<3000$ gauss and for gas densities less than 0.15 g/cm³ the effect of the λ' transitions on the quenching is negligible and that, in fact, the quenching is given by Eq. (1) with r_0 replaced by $r=r_0/(1+r_0\lambda)$.

In order to obtain an experimental value for r_0 and to check v, we make the definite assumption that λ' transitions are negligible. For each density we then determine the best value for r, using only data with $H<3000$ gauss. Consequently, the plot shown in Fig. 2 should be linear. The probable errors are large because $1/r$ is relatively sensitive to n; a one percent change in n produces at least a six percent change in $1/r$. The intercept and slope of the least squares line fitted to the data give the values of r_0 and σ. Our procedure requires only that Siegel and De Benedetti's value of σ be correct as to order to magnitude, justifying neglect of the λ' transitions; in this sense only is our value of σ independent. In computing σ from λ, we have assumed the dominance of single collisions. We find $r_0=1050\pm140$ compared with Ore and Powell's theoretical result of $r_0=1120$, and we find $\sigma=8\times10^{-22}$ cm² compared with $\sigma=10^{-21}$ cm² obtained by Siegel and De Benedetti.[9]

* Work done in Sarah Mellon Scaife Radiation Laboratory. Support of the ONR is acknowledged.
† Now at the University of Illinois, Urbana, Illinois.
[1] J. Wheatley and D. Halliday, Phys. Rev. **87**, 235 (1952).
[2] M. Deutsch and E. Dulit, Phys. Rev. **84**, 601 (1951).
[3] T. A. Pond and R. H. Dicke, Phys. Rev. **85**, 489 (1952).
[4] S. De Benedetti and R. Siegel, Phys. Rev. **85**, 377 (1952).
[5] R. Drisko, private communication.
[6] A. Ore and J. L. Powell, Phys. Rev. **75**, 1696 (1949).
[7] M. Deutsch and S. C. Brown, Phys. Rev. **85**, 1047 (1952).
[8] O. Halpern, Phys. Rev. **88**, 232 (1952).
[9] R. Siegel and S. De Benedetti, Phys. Rev. **87**, 235 (1952).

Reprinted from THE PHYSICAL REVIEW, Vol. 88, No. 6, 1291-1295, December 15, 1952
Printed in U. S. A.

Energy Levels in Light Nuclei*

J. C. ARTHUR,† A. J. ALLEN, R. S. BENDER H. J. HAUSMAN,‡ AND C. J. MCDOLE§
University of Pittsburgh, Pittsburgh 13, Pennsylvania

(Received July 21, 1952)

Targets of beryllium, Nylon, lead fluoride, sulfur, and lead sulfide were bombarded with 8 Mev protons from the University of Pittsburgh cyclotron. Energy levels were observed in Be^9, C^{12}, N^{14}, O^{16}, F^{19}, and S^{32} by inelastic scattering at 150° from thin targets. Single levels were assigned in Be^9 and C^{12}; two levels were assigned in N^{14}; nine levels were assigned in F^{19}; and seven levels were assigned in S^{32}.

I. INTRODUCTION

THE present investigation was undertaken to look for additional low-lying levels in some light nuclei. Similar work has been done at this laboratory by Ely *et al.*,[1] Reilley *et al.*,[2] and Hausman *et al.*[3] The 8-Mev proton beam from the University of Pittsburgh cyclotron was used to bombard targets of beryllium, Nylon, fluorine, and sulfur. The incident and reaction particle momenta were analyzed magnetically. Inelastic scattering was used to determine energy levels in Be^9, C^{12}, N^{14}, O^{16}, F^{19}, and S^{32}.

II. APPARATUS

The apparatus used is essentially the same as that described previously.[4,5] It was modified by placing the detector inside the vacuum system to permit the observation of lower energy scattered particles. The target holder was remodeled to provide a means for calibration of the reaction particle analyzer without losing the vacuum.

A beam of 8-Mev protons from the cyclotron was focused by a sector magnet into a shielded scattering room. Within the scattering room the incident beam was analyzed magnetically by a 40° sector magnet and the spread in energy adjusted by appropriate slits. Charged reaction particles were momentum analyzed by a 60° sector magnet and detected by a scintillation counter using a ZnS crystal. Both analyzing magnets were calibrated with polonium alpha-particles using

* Work done in the Sarah Mellon Scaife Radiation Laboratory and assisted by the joint program of the ONR and AEC.
† Now at Project Lincoln, Massachusetts Institute of Technology, Cambridge, Massachusetts.
‡ Now at the Ohio State University, Columbus, Ohio.
§ AEC Predoctoral Fellow.
[1] Ely, Allen, Arthur, Bender, Hausman, and Reilley, Phys. Rev. 86, 859 (1952).
[2] Reilley, Allen, Arthur, Bender, Ely, and Hausman, Phys. Rev. 86, 857 (1952).
[3] Hausman, Allen, Arthur, Bender, and McDole, following paper [Phys. Rev. 88, 1296 (1952)].
[4] Bender, Reilley, Allen, Ely, Arthur, and Hausman, Rev. Sci. Instr. 23, 542 (1952).
[5] University of Pittsburgh Radiation Laboratory Precision Scattering Report No. 2, May (1952) (unpublished).

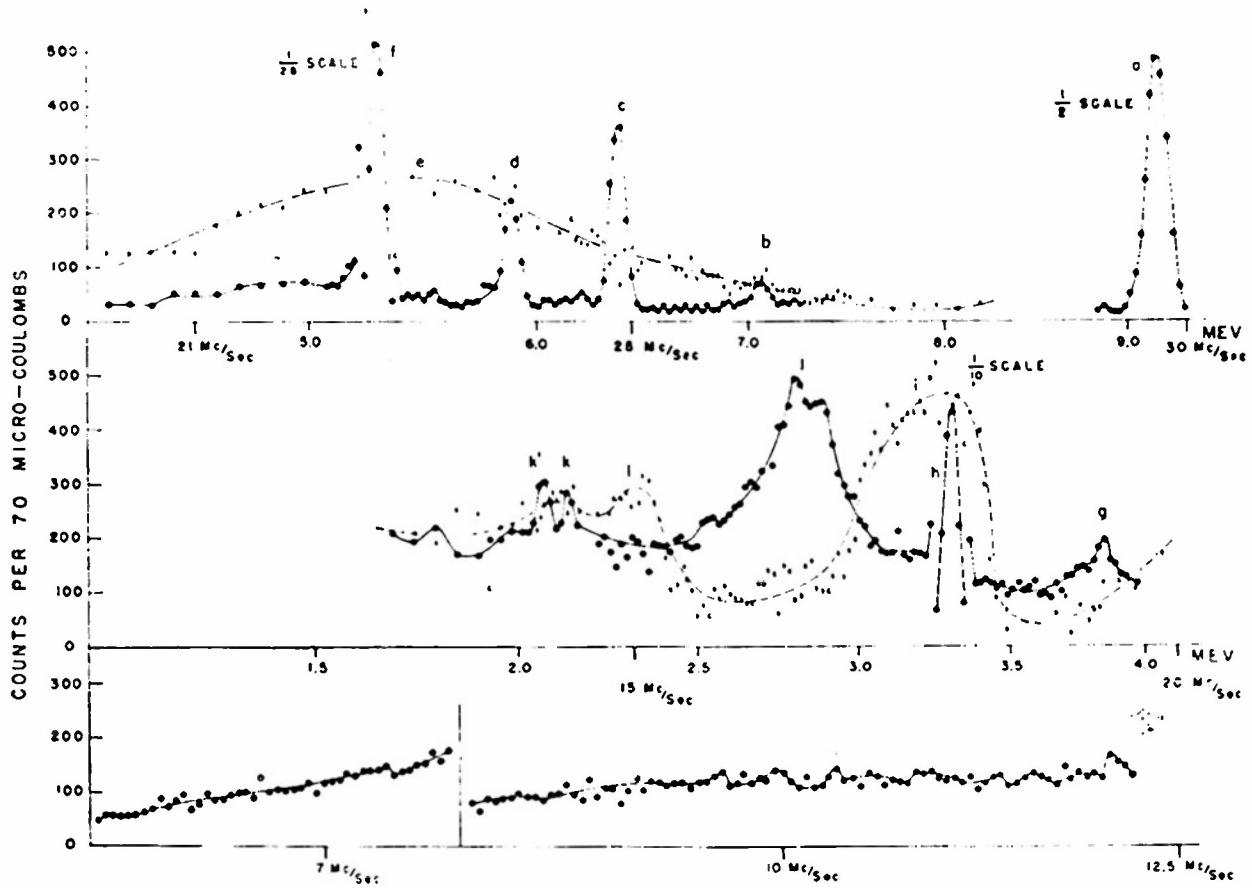

FIG. 1. Spectrum of charged particles scattered from beryllium at 150°.

$H\rho = 3.3159 \times 10^8$ gauss-cm.[6] Magnetic field strength measurements were made with proton resonance detectors. The analyzing magnets were carefully demagnetized before each run. The incident beam current was integrated to 70 microcoulombs (30 microcoulombs for one S^{32} bombardment) for each setting of the magnet which analyzed the scattered particles. The spread in incident energy was 0.04 Mev during the experiment with the beam incident perpendicularly on the target. At least two bombardments of each element were made using different targets where possible.

III. EXPERIMENTAL PROCEDURE AND DISCUSSION

A. Be^9 + Proton

Beryllium targets of 0.2 mg/cm² and 0.3 mg/cm² were bombarded with protons and the reaction particles studied at 150° with respect to the incident beam. Figure 1 shows a plot of the number of counts per 70 microcoulombs of charge collected vs proton resonance frequency in Mc/sec at which reaction particles were detected. Peaks *b*, *c*, *d* and *f* are due to elastic scattering from Al^{27}, O^{16}, C^{12}, and Be^9. Peak *h* is from the known excited level in Be^9 at 2.4 Mev. The average value of excitation energy obtained for this level from two runs is 2.44 Mev, which is to be compared with the values of 2.422±0.005 Mev determined by Van Patter *et al.*[6] and 2.433±0.005 Mev determined by Browne *et al.*[7] No new levels were found in Be^9 for an excitation energy of 6 Mev.

Peaks *a*, *e*, *g*, and *j* have been identified as deuterons from the reaction $Be^9(p,d)Be^8$ corresponding to the ground state and energy levels in Be^8 at 2.8, 4.0, and 5.1 Mev, respectively.

Peaks *i* and *l* are alpha-groups from the $Be^9(p,\alpha)Li^6$ reaction corresponding to the ground state and excited levels in Li^6 at 2.1 Mev (for a bibliography see Hornyak *et al.*,[8] hereafter referred to as HFML). The peaks *k* and *k'* are attributed to inelastic protons from the 4.4-Mev level in C^{12} which appears as a surface contaminant on the front and back of the target.

Peaks *e*, *i*, and *l* were obtained by subtraction of the readings taken with a foil in front of the detector from readings taken without a foil.

B. Nylon + Proton

Nylon targets of surface density 0.50 mg/cm² were bombarded by 8-Mev protons. The reaction particles

[6] Van Patter, Sperduto, Huang, Strait, and Buechner, Phys. Rev. 81, 233 (1951).

[7] Browne, Williamson, Craig, and Donahue, Phys. Rev. 83, 179 (1951).

[8] Hornyak, Lauritsen, Morrison, and Fowler, Revs. Modern Phys. 22, 309 (1950).

were analyzed at 90° and 150°. Peaks *a*, *b*, c_1, and *c* of Fig. 2 are elastically scattered protons from O^{16}, N^{14}, C^{13}, and C^{12}, respectively. Peak *f* is the only excited state obtained in C^{12} for an excitation energy of 6.5 Mev. An excitation energy of 4.45 Mev was determined for this level. This is an average value obtained from four Nylon bombardments and nine other bombardments where carbon was a surface contaminant. The width of the peak is thought to be caused mainly by target thickness. A fresh target was used for the data yielding peak *f* Fig. 2 in an attempt to reduce the probability of target deterioration causing a widening of the peak. Many previous investigations of C^{12} have been made (see HFML, p. 325). The most accurately known value for this energy level is 4.438±0.014 Mev obtained by magnetic analysis.[8]

Three levels and possibly a fourth were found in N^{14} from the reaction $N^{14}(p,p')N^{14*}$. Peaks *d*, *e*, and *g* of Fig. 2 correspond to energy levels of 2.32, 3.96, 5.09 Mev. If e_1 were a peak in N^{14} the value of the energy level would be 3.76 Mev. Since a C^{13} elastic peak was observed it is possible that it is an energy level of this isotope.[‖] Its excitation energy in C^{13} would be 3.69 Mev. A level in C^{13} is known to exist at 3.677±0.005 Mev.[9] Previous investigations on N^{14} energy levels were made by Thomas and Lauritsen[9] giving values of 1.643±0.004, 2.318±0.008, 3.390±0.010, 3.92, 5.056±0.025 Mev; by Burrows *et al.*[10] giving values of 3.95 and 5.06 Mev; and by Heydenburg *et al.*[11] giving levels at 2.35 and 3.95 Mev. Thomas and Lauritsen observed gamma-rays resulting from bombarding an enriched C^{13} target with deuterons. The gamma-ray energies which they assigned as energy levels in N^{14} at 1.6 Mev and 3.4 Mev have since been attributed to cascading gamma-rays (private communication with T. Lauritsen).

Peaks *h* and *i* are assigned to the oxygen doublet at 6.0 and 6.1 Mev. The best information about the doublet which can be calculated from the Nylon, PbS, and PbF_2 data (oxygen appeared as a contaminant on the last two targets) is a value of 0.087±0.010 Mev for the doublet separation. Previous measurements of these levels and their separation have been made by Chao *et al.*[12] They give values of 6.052, 6.136, and 0.084±0.006 Mev for the energy levels of the two peaks and their separation, respectively. Several other measurements of these levels have been made (see HFML, p. 343).

C. F^{19}+ Proton

A target of PbF_2(1.20 mg cm^{-2}) was evaporated on a gold backing. With 8-Mev protons incident on the

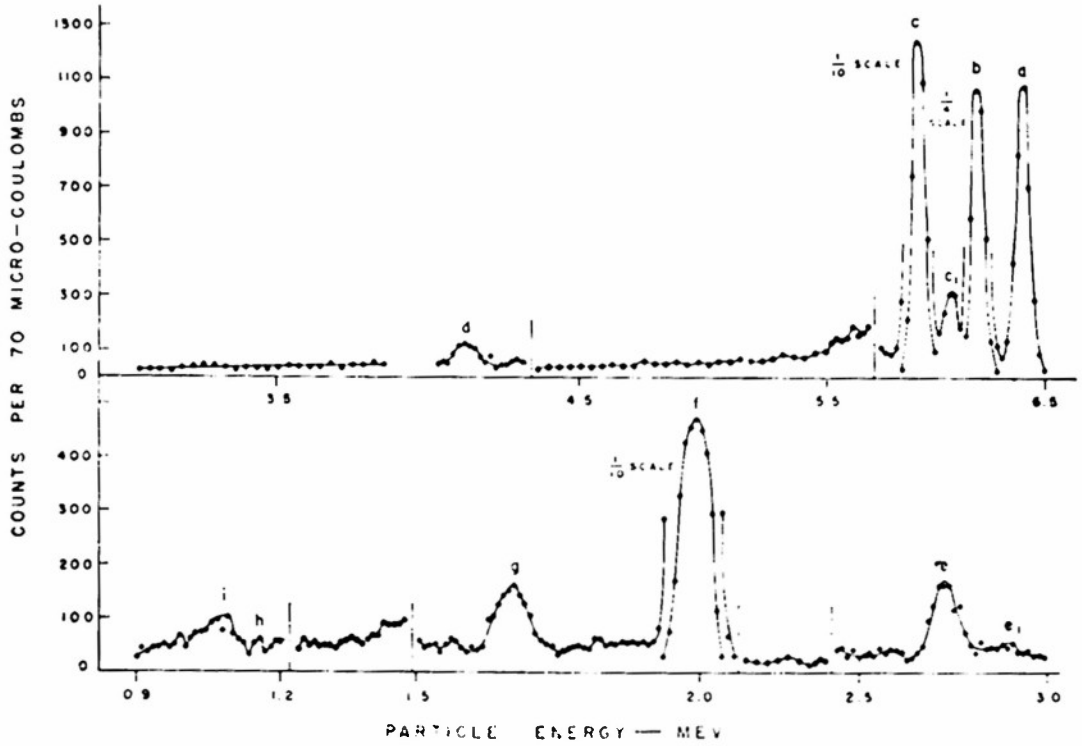

FIG. 2. Spectrum of charged particles scattered from Nylon at 150°.

‖ *Note added in proof:* Further work indicates that this level is from C^{13}.

[8] R. G. Thomas and T. Lauritsen, Phys. Rev. **78**, 88 (1950).
[10] Burrows, Powell, and Rotblat, Proc. Roy. Soc. **A209**, 478 (1951).
[11] Heydenburg, Phillips, and Cowie, Phys. Rev. **85**, 742 (1952).
[12] Chao, Toliestrup, Fowler, and Lauritsen, Phys. Rev. **79**, 108 (1950).

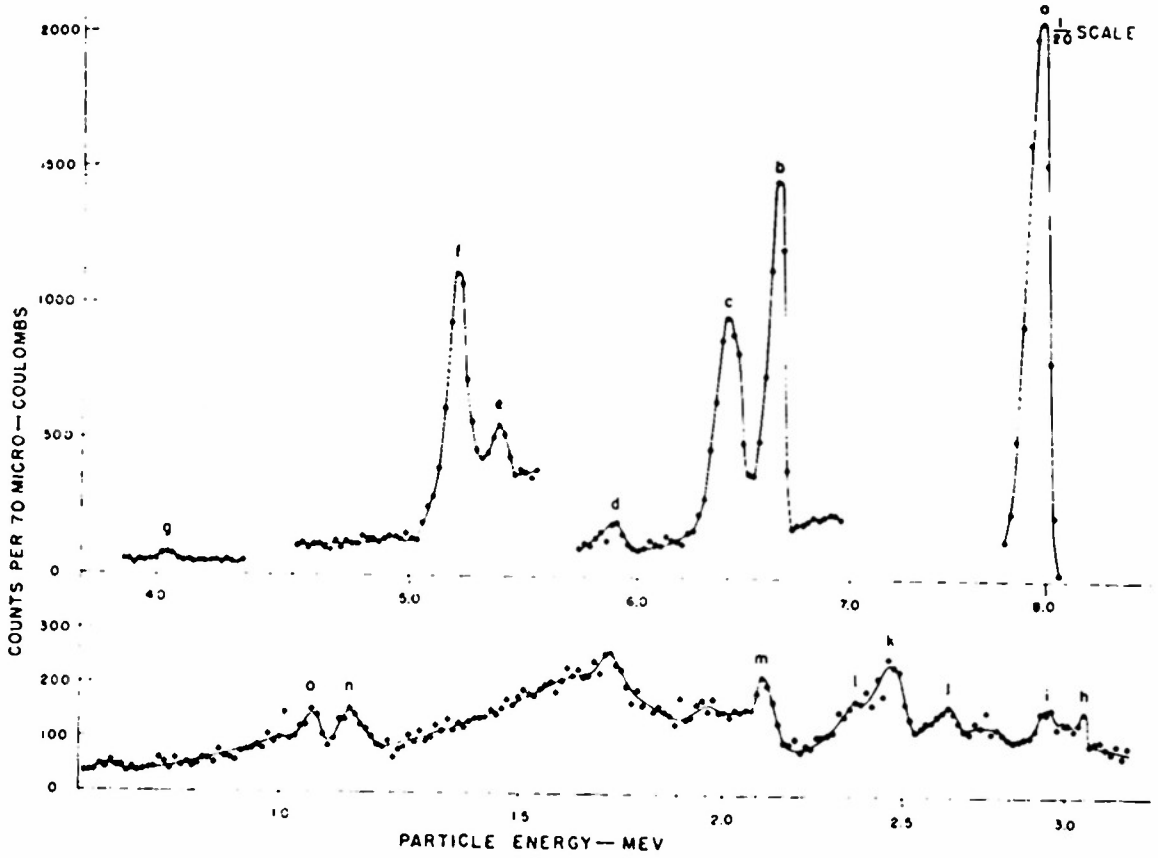

FIG. 3. Spectrum of charged particles scattered from fluorine at 150°.

target protons from the reaction $F^{19}(p,p')F^{19*}$ were observed at 150°. Figure 3 shows sections of each of two bombardments. Peak *a* is a group of protons elastically scattered from lead and gold. Peaks *b*, *c*, and *d* are the elastic peaks of F^{19}, O^{16}, and C^{12}, respectively. Peaks *e*, *f*, *g*, *h*, *i*, *j*, j_1, *k*, and *l* correspond to energy levels in F^{19} at 1.37, 1.59, 2.82, 3.94, 4.06, 4.41, 4.48, 4.59, and 4.76. Peak j_1 is not shown as a peak in Fig. 3. Peak *m* is the excited state in C^{12} at 4.4 Mev. Peaks *n* and *o* are the 6.0- and 6.1-Mev levels in O^{16}. No other levels of comparable intensity were observed for an excitation energy of 6.7 Mev. There were indications of seven other possible energy levels: one each at 4 and 4.3, three near 4.6, and two near 4.8 Mev, each of which reproduced on the two bombardments. A bibliography of previous investigations of energy levels of F^{19} is given by HFML, p. 353. Recently, Bullock and Sampson[13] found energy levels at 1.36±0.05, 2.76 ±0.05, 3.92±0.05 Mev; Heydenburg, Phillips, and Cowie[32] found levels at 1.53, 3.83 Mev, and Shull[14] found a level at 1.52 Mev. No attempt was made to study the reaction $F^{19}(p,\alpha)O^{16*}$. The spectrum shown in Fig. 3 is taken with the alpha-groups removed by placing aluminum foils in front of the detector. A broad peak appears between 1 and 2 Mev. This is a proton group which appeared on a bombardment of the gold backing made under similar conditions. It is thought to be due to (p,p') reactions in copper or silver known to exist in the gold in quantities less than 0.2 percent. All peaks shown in Fig. 3 were observed on two bombardments of the same target; however, the values above were calculated from the second run only.

D. S^{32} + Proton

The $S^{32}(p,p')S^{32}$ reaction was studied by bombarding targets of lead sulfide and sulfur on gold. A spectrum of the reaction particles in the 150° direction obtained by bombarding S^{32} with 8-Mev protons is shown in Fig. 4. *a*, *b*, and *c* are the elastic peaks of Au^{197}, S^{32}, and O^{16}, respectively. Peaks *e*, *f*, *g*, *h*, *i*, *j*, and *n* are assigned to excited levels in S^{32} at 2.25, 3.81, 4.32, 4.50, 4.74, 5.04, and 5.83 Mev, respectively. Peaks *k* and *l* are attributed to the 4.4-Mev level in C^{12} and result from carbon contaminants on the target surfaces. Four peaks (*d*, d_1, *m*, and *o*) were not used for calculations. In previous studies of S^{32} (see Alburger and Hafner[33]) excited levels were observed at 2.25 and 4.34 Mev.

[13] M. L. Bullock and M. B. Sampson, Phys. Rev. 81, 967 (1951).
[14] F. B. Shull, Phys. Rev. 83, 875 (1951).

[33] D. E. Alburger and E. M. Hafner, Revs. Modern Phys. 22, 379 (1950).

IV. RESULTS AND ERRORS

Table I is a list of the elements studied and the energy levels obtained. In all (p,p') reactions, except F^{19}, where three figures are quoted an estimate of the probable error is 0.02 Mev (for F^{19} the estimated probable error is 0.03 Mev). The primary contribution to this probable error is due to an uncertainty in the calibration of the magnetic field strength of the reaction particle analyzer. This uncertainty arises from a nonlinearity between the ratio of the measured field strength to the fringing field strength and the measured field strength and also from hysteresis effects. There are indications, in general, that the levels are higher than previously published values of the same levels where the accuracy quoted is of the order of 0.01 Mev.

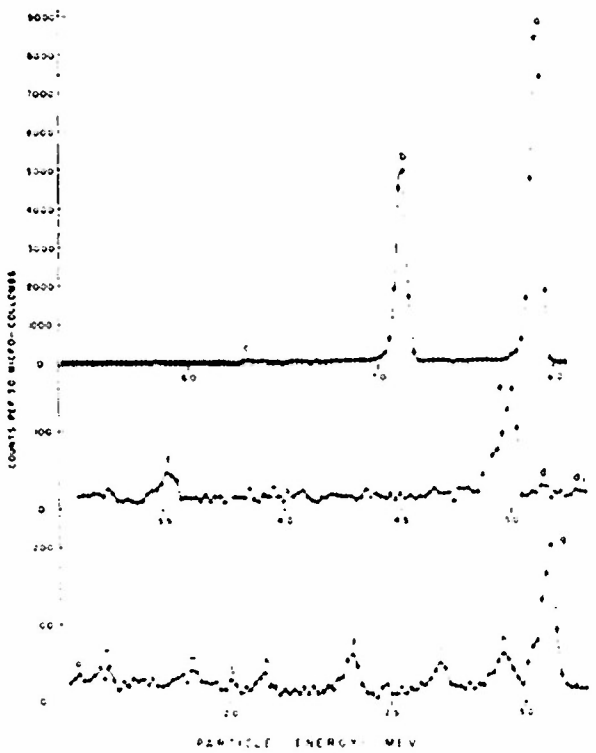

FIG. 4. Spectrum of charged particles scattered from sulfur at 150°.

TABLE I. Energy levels in Be^9, N^{14}, O^{18}, F^{19}, and S^{32}.

Element	Energy level (Mev)	Doublet separation (Mev)
Be^9	2.44	
C^{12}	4.45	
N^{14}	2.32	
	3.76?	
	3.96	
	5.09	
O^{18}	6.0	0.087
	6.1	
F^{19}	1.37	
	1.59	
	2.82	
	3.94	
	4.06	
	4.41	
	4.48	
	4.59	
	4.76	
S^{32}	2.25	
	3.81	
	4.32	
	4.50	
	4.74	
	5.04	
	5.83	

The authors wish to thank L. M. Diana, K. B. Rhodes, R. F. Weise, R. A. Barjon, Miss C. Gegauff, and E. M. Perkins for their many contributions to this project.

Integral Equation for Stripping

E. Gerjuoy

This subject has been discussed recently by Austern[1] who has attempted to clarify the agreement between the results obtained from Butler's theory[2] and from Born approximation.[3] Austern's conclusions are drawn from an integral equation for the wave function of the problem, in which the Green's function is expressed in momentum space. We shall show that the integral equation can be more readily interpreted if the Green's function is written in coordinate space, and that in Austern's equation (6) the term $\langle \psi_j e^{i\mathbf{R}\cdot\mathbf{k}_p} | V_{Ns} - V_{NP} | \varphi_i \psi_D \rangle$ makes a vanishing contribution to the scattering amplitude. This result modifies his demonstration that the terms in V_{NP} are cancelled when his Ψ is replaced by $\varphi_i \psi_D$. Our own point of view on the connection between the Born approximation[3] and Butler's theory[2] will be presented in another report, to which the present report is preliminary.

1. N. Austern, Phys. Rev. 89, 318 (1953)

2. S. T. Butler, Proc. Roy Soc. Lond. A208, 559 (1951)

3. I. B. Daitch and J. B. French, Phys. Rev. 87, 900 (1952)

We regard the initial nucleus as a fixed center of force of spin zero (as do Daitch and French[3]), thereby obviating the need for internal nuclear coordinates. The Hamiltonian is

$$H = T_N + T_p + V_N + V_p + V_{NP} \qquad (1)$$

where T represents kinetic energy, V_N and V_p are the interactions of neutron and proton respectively with the fixed center of force, and V_{NP} is the neutron-proton interaction. The solution Ψ obeys the integral equation

$$\Psi = \Psi_0 - G(V_P + V_{NP})\Psi \tag{2}$$

where

$$(T_N + T_P + V_N - E)\Psi_0 = 0 \tag{3a}$$

$$(T_N + T_P + V_N - E)G = I \tag{3b}$$

I is the unit operator in the configuration space of neutron-proton coordinates and spin. G is the outgoing Green's function, given by

$$G = \sum_\lambda g_P(E-\lambda)\varphi_N(r_N, \Delta_N, \lambda)\varphi_N^*(r_N', \Delta_N', \lambda) \tag{4}$$

Δ denotes spin coordinates, and $\varphi_N(\lambda)$ are the complete set of eigenfunctions of the neutron in the field of the initial nucleus

$$(T_N + V_N - \lambda)\varphi_N(\lambda) = 0 \tag{5}$$

$g_p(E-\lambda)$ is the outgoing Green's function for the proton in free space (and spin), i.e.

$$(T_P - E + \lambda)g_P = I_P \tag{6}$$

with I_p the unit operator in proton coordinate and spin space.

Since in momentum space the representation of g_p is proportional to $\left[-\hbar^2K^2/2M - E + \lambda\right]^{-1}$, Austern's integral equation (6) is seen to be in our notation

$$\Psi = \Psi_D - G(V_N - V_{NP})\Psi_D - G(V_P + V_{NP})\Psi \tag{7}$$

where, as previously,[1] Ψ_D represents a plane wave of free deuterons.

The boundary conditions on the problem are that the wave function is incident as a deuteron at infinity (far from the center of force), but is

otherwise everywhere outgoing. Thus equations (2) and (3a) imply that Ψ_0 is a combination of free space proton functions and of neutron functions $\varphi_N(\lambda)$ which at infinity looks like an incoming plane wave of free deuterons, but in which the neutrons and protons propagate independently of each other, since V_{NP} does not appear in equation (3a). Except for the incoming part Ψ_D, Ψ_0 must be everywhere outgoing at infinity. Equations (2) and (7) presumably represent the same Ψ, implying we should be able to show

$$\Psi_0 = \Psi_D - G(V_N - V_{NP})\Psi_D \tag{8}$$

Using

$$(T_N + T_P + V_{NP} - E)\Psi_D = 0 \tag{9}$$

and equation (3b) it is seen that

$$(T_N + T_P + V_N - E)[\Psi_D - G(V_N - V_{NP})\Psi_D] = 0 \tag{10}$$

Thus the right and left sides of equation (8) satisfy the same differential equation, equations (3a) and (10), and also satisfy the same boundary conditions, namely they are everywhere outgoing at infinity except for identical incoming terms Ψ_D. This is sufficient to prove that both sides of equation (8) represent the same function. Equation (8) can also be established directly from equation (9), rewritten in the form

$$(T_N + T_P + V_N - E)\Psi_D = (V_N - V_{NP})\Psi_D \tag{11}$$

Since Ψ_0 and Ψ_D have identical incoming terms, equation (11) using equation (3) is equivalent to the integral equation

$$\Psi_D = \Psi_0 + G(V_N - V_{NP})\Psi_D \tag{12}$$

which is equation (8). The identity of equation (2) with Austern's equation (6), our equation (7), has thereby been demonstrated.

That in (d,p) reactions the term G ($V_N - V_{NP}$) makes a vanishing contribution to the scattering amplitude now can be seen on physical grounds, recalling the interpretation of Ψ_0 . Only continuum (positive λ) eigenfunctions can come in from infinity. In order that the neutron be captured therefore, it is necessary that the proton remove the excess neutron energy. But, as pointed previously, equation (3a) for Ψ_0 contains no neutron-proton coupling term. Consequently Ψ_0 cannot yield neutron capture.

This plausible argument is made rigorous as follows. The number of scattered protons which reach infinity with polarization τ , while leaving the neutron in a bound state of energy λ_f, total angular momentum j, and magnetic quantum number m, is determined from

$$\lim_{r_p \to \infty} \int d\vec{r}_N \sum_{\Delta_N, \Delta_P} \chi^{\tau *}(\Delta_P) \varphi_{Nj}^{m *}(r_N, \Delta_N, \lambda_f) \Psi(r_P, r_N, \rho_P, \Delta_N) \quad (13)$$

In (13) $\chi^\tau = \chi^\pm$ is the proton spin function. Substituting equation (7) in equation (13), the term in Ψ_D vanishes exponentially as $r_p \to \infty$ since $\varphi_N(\lambda_f)$ is a bound state. The terms in G lead in the usual way, via equation (4) and the orthonormality of the set $\varphi_N(\lambda)$, to the scattering amplitude $A(\vec{n})$ of the protons along the direction n, $A(\vec{n})$, the coefficient in (13) of r_p^{-1} exp (i k r_p) as $\vec{r}_p \to \infty$ along $\vec{n}$, is

$$A(\vec{n}) = A_1(\vec{n}) + A_2(\vec{n}) \quad (14)$$

$$A_1(\vec{n}) = -\frac{1}{4\pi} \frac{2M}{\hbar^2} e^{-ik \cdot r_p} \chi^{\tau *}(\Delta_P) \varphi_{Nj}^{m *}(r_N, \Delta_N, \lambda_f)(V_N - V_{NP}) \Psi_D \quad (15a)$$

$$A_2(\vec{n}) = -\frac{1}{4\pi} \frac{2M}{\hbar^2} e^{-ik \cdot r_p} \chi^{\tau *}(\Delta_P) \varphi_{Nj}^{m *}(r_N, \Delta_N, \lambda_f)(V_P + V_{NP}) \Psi \quad (15b)$$

In equation (15) V_N, V_P, and V_{NP} operate to the right, and summation over s_P, s_N and integration over all r_P, r_N is implied. $\vec{k} = k\vec{n}$ and $\frac{\hbar^2 K^2}{2M} = E - \lambda_f$ with M the mass of proton or neutron. The function Ψ_D is

$$\Psi_D = e^{iK\cdot(r_P + r_N)/2} w(r_P - r_N, \beta_P, \beta_N) \tag{16}$$

w is the wave function of the deuteron in its ground state, with specified magnetic quantum number. In other words, letting $r_P - r_N = r$,

$$\left(-\frac{\hbar^2}{M}\Delta_r + V_{NP} - \epsilon\right) w = 0 \tag{17}$$

with ϵ the energy of the deuteron in its ground state, and $\frac{\hbar^2 K^2}{4M} = E - \epsilon$.

In equation (15a) V_N is Hermitian, and does not involve r_P or s_P. Hence, from equation (5), and using also equations (16) and (17) to eliminate V_{NP}, equation (15a) becomes

$$A_1(\vec{n}) = B_1(\vec{n}) - B_2(\vec{n}) \tag{18}$$

$$B_1(\vec{n}) = -\frac{1}{4\pi}\frac{2M}{\hbar^2} e^{-ik\cdot r_P} \chi^{\tau *}(\beta_P)\left[(\lambda - T_N)\varphi_{Nj}^{m}(\lambda_f)\right]^{*} \Psi_D \tag{19a}$$

$$B_2(\vec{n}) = -\frac{1}{4\pi}\frac{2M}{\hbar^2} e^{-ik\cdot r_P} \chi^{\tau *}(\beta_P)\varphi_{Nj}^{m*}(\lambda_f) e^{iK(r_P + r_N)/2}\left[(\epsilon + \frac{\hbar^2}{M}\Delta_r) w\right] \tag{19b}$$

We introduce $r = r_P - r_N$ as a new independent variable, replacing r_P, in equations (19), and observe that because $\varphi_{Nj}^{m}(\lambda_f)$ and w are bound states, integration by parts, so as to cause $T_N = -\frac{\hbar^2}{2M}\Delta_N$ and $\frac{\hbar^2}{M}\Delta r$ to operate on the exponential functions, is legitimate. There result

$$B_1(\vec{n}) = -\frac{1}{4\pi}\frac{2M}{\hbar^2}\chi^{\tau *}(\beta_P) w(\vec{r}) e^{ir\cdot(\frac{K}{2} - k)} \varphi_{Nj}^{m*}(r_N, \lambda_f)\left[(\lambda_f + \frac{\hbar^2}{2M}\Delta_N) e^{ir_N\cdot(K-k)}\right] \tag{20a}$$

$$B_2(\vec{n}) = -\frac{1}{4\pi}\frac{2M}{\hbar^2}\chi^{\tau *}(\beta_P) w(\vec{r})\left[(\epsilon + \frac{\hbar}{M}\Delta_r) e^{ir\cdot(\frac{K}{2} - k)}\right] \varphi_{Nj}^{m*}(r_N, \lambda_f) e^{ir_N\cdot(K-k)} \tag{20b}$$

Equations (20) imply of course integration over all r and r_N. Performing the indicated differentiation and recalling the definitions of K and k, we find that $B_1(n) = B_2(n)$.

This completes the proof that $A_1(\vec{n})$, eq.(15a), the portion of the

scattering amplitude resulting from the term $G(V_N - V_{NP})\Psi_D$ in eq. (7) is zero. The scattering amplitude is given solely by $A(\vec{n}) = A_2(\vec{n})$, eq (15b). It will be noted that in this demonstration there was no need to assume w spherically symmetric, nor was V_{NP} assumed central or spin-independent.

Replacing Ψ by Ψ_D in equation (15b) permits V_{NP} to be replaced by V_N in that equation, since $A_1(n)$, equation (15a), has been proved equal to zero. This yields the starting point of Daitch and French.[3] Judging by equation (2), it is equally natural to regard Ψ_0 as the solution in the absence of scattering, suggesting that it might be more accurate to replace Ψ in equation (15b) by Ψ_0. However we shall not pursue this point in this report.

B. Bergquist

Physics Department, University of Pittsburgh.

1. Introduction

The theory of (d,p) and (d,n) reactions given by Butler[1] has been the subject of a number of theoretical papers.[2-6]

---

1. S. T. Butler, Proc. Roy. Soc. Lond. A 208, 559 (1951)
2. A. B. Pratt a et al., Phil. Mag. 43, 485 (1952)
3. P. B. Daitch and J. A. French, Phys. Rev. 87, 900 (1952)
4. R. Huby, Proc. Roy. Soc. Lond. A 215, 385 (1952)
5. N. Austern, Phys. Rev. 89 318, (1953)
6. F. Friedman and W. Tobocman, "An Approximate Wave Mechanical Description of Deuteron Stripping", to be published.

Butler's original deduction of the angular distribution in stripping involved fitting together at the nuclear radius the solutions interior and exterior to the nucleus [illegible] fair to call complicated the procedure by which Butler obtained the cross section from his solution. Succeeding theoretical studies have been of two kinds; (a) attempts

*Work done in part at the Sarah Mellon Scaife Radiation Laboratory and assisted by the Joint Program of the Office of Naval Research and the Atomic Energy Commission.

to simplify and clarify Butler's calculation of the cross section, but retaining his basic idea of fitting together the interior and exterior solutions[4,6] and (b) assuming the Born approximation matrix element for the reaction after which Butler's formula is obtained by more or less direct integration.[2,3] Since Butler's calculation does not seem equivalent to Born approximation it is somewhat surprising that Born approximation gives Butler's results.[3] Austern[5] has attempted to explain this agreement.

In subsequent sections we shall rederive Butler's result by means of standard Green's function techniques, thereby automatically and obviously satisfying the boundary conditions at infinity and at the nuclear radius. To minimize formal complications we consider the following idealization of the stripping problem: A deutron, spinless, composed of spinless neutron and proton, impinges on a fixed center of force which is the initial nucleus.[3] At infinity the solution Ψ must be of the form

$$\Psi = \psi_D + \Phi \qquad (1)$$

where ψ_D is the incident plane wave of deuterons on the initial nucleus, and Φ is everywhere outgoing. In the problem at hand this means: Let the energy have a positive imaginary part; then Φ is everywhere outgoing if it remains bounded as r_N or r_p or both approach infinity. We have been careful to obtain the cross section by a mathematical

procedure which corresponds evidently to the experimental situation. To amplify this remark, denote the wave function of the final nucleus in a (d,p) reaction, in which the neutron is captured into a bound state, by $\varphi(\vec{r}_N)$. Then the probability of finding the proton at $\vec{r}_p$, with the neutron bound in its final state, is $|\int d\vec{r}_N \varphi^*(\vec{r}_N)\Psi(\vec{r}_N,\vec{r}_p)|^2$ The experiment measures the flux at infinity of protons whose energy corresponds to leaving the neutron in state $\varphi(\vec{r}_N)$, which flux per unit solid angle is $(\hbar k/M)|A(\vec{n})|^2$ where the scattering amplitude A(n) in the direction $\vec{n}$ is given by

$$A(\vec{n})\frac{e^{ikr_p}}{r_p} = \lim_{r_p\to\infty}\int d\vec{r}_N \varphi^*\Psi \qquad (2)$$

and $\vec{r}_N$ approaches infinity along $\vec{n}$.
We always employ the definition eq. (2) of $A(\vec{n})$ to evaluate the cross section.

Using eq. (2) in the integral equation for the problem leads in a very straightforward way to the Born approximation matrix element, for which no satisfactory justification has been given previously. In so doing we illuminate the reason for the agreement between the two seemingly different methods (a) and (b) above. Our integral equation is the same as that obtained by Austern[5], but his not using the definition (2) for the scattering amplitude caused him to overlook the fact that not all the terms in his equation yield protons at infinity, in (d,p) reactions. This statement will be further amplified below. Finally we append some discussion concerning the success of the theory.

II. The Integral Equation

We fix our attention on (d,p) reactions, i.e. we seek outgoing protons whose energy corresponds to leaving the neutron bound to the center of force. The Hamiltonian is

$$H = T_N + T_P + V_P + V_N + V_{NP} \tag{3}$$

where T represents kinetic energy, V_N and V_P are the interaction of neutron and proton respectively with the fixed center of force, and V_{NP} is the neutron proton interaction[7]

---

7. The discussion and notation of this section parallels that in E. Gerjuoy "Integral Equation for Stripping", University of Pittsburgh Precision Scattering Project Report #3.

The solution satisfies

$$(H-E)\Psi = 0 \tag{4}$$

with Ψ of the form eq. (1) and

$$\psi_D = e^{i\vec{K}\cdot(\vec{r}_P+\vec{r}_N)/2}\, w(\vec{r}_P - \vec{r}_N) \tag{5}$$

w is the ground state of the deuteron, ψ_D satisfies

$$(T_N + T_P + V_{NP} - E)\psi_D = 0 \tag{6}$$

Using an obvious symbolic notation, the solution satisfies the integral equation

$$\Psi = \psi_0 - G(V_P + V_{NP})\Psi \tag{7}$$

where

$$(T_N + T_P + V_N - E)\psi_0 = 0 \qquad (8)$$

$$(T_N + T_P + V_N - E)G = 1 = \delta(\vec{r}_P - \vec{r}_P')\,\delta(\vec{r}_N - \vec{r}_N') \qquad (9)$$

The solution to eq. (7) satisfies the boundary conditions at the nuclear radius, and satisfies the boundary condition at infinity if G is the outgoing Green's function, which is[3]

---

8. It is apparent that G, eq. (10), satisfies eq. (9) and is outgoing in the protons, in the sense which has been explained in the previous section. It is possible to prove that G is also outgoing in the neutrons, despite the fact that it seems to contain, through $\varphi(\vec{r}_P)$, both incoming and outgoing spherical waves in $\vec{r}_N$. It must be granted that some mathematical questions concerning the proof are not altogether settled, but its essential correctness seems established. The proof is contained in a report in preparation by B. Friedman and L. Gerjuoy, on the subject of many particle scattering problems. Related problems are discussed in B. Friedman and L. Gerjuoy, Research Report # CX-4, and in Harry L. Moses, Research Report #CX-5, both issued by New York University, Washington Square College of Arts and Science Mathematics Research Group.

$$G(\vec{r}_P, \vec{r}_P'; \vec{r}_N, \vec{r}_N') = \sum_\lambda g(\epsilon - \lambda)\varphi^*(\vec{r}_N, \lambda)\varphi(\vec{r}_N', \lambda) \qquad (10)$$

In eq. (10) the sum over λ includes an integration in the continuum $\lambda > 0$. $\varphi(\lambda)$ are the complete set of eigenfunctions of the neutrons in the field of the initial nucleus

$$(T_N + V_N - \lambda)\varphi(\lambda) = 0 \tag{11}$$

$g(E-\lambda)$ is the outgoing free space Green's function for the proton[9], i.e.

$$(T_p - E + \lambda) g(E-\lambda) = \delta(\vec{r}_p - \vec{r}_p') \tag{12}$$

$$g(\vec{r}_p - \vec{r}_p') = \frac{1}{4\pi}\frac{2M}{\hbar^2}\frac{e^{i\sqrt{E-\lambda}\,|\vec{r}_p - \vec{r}_p'|}}{|\vec{r}_p - \vec{r}_p'|} \tag{13}$$

In eq. (13) M is the mass of proton or neutron and $\mathrm{Re}\sqrt{E-\lambda} > 0$ when E is imaginary.

---

9. In order that eqs. (10) and (12) yield a convergent result in eq. (7), Coulomb forces must be neglected or replaced by screened fields. We are also ignoring some formal difficulties connected with the fact that V_{NP} is a function of $\vec{r}_p - \vec{r}_N$ only, and does not approach zero along all radii of an infinite sphere in the six dimensional $\vec{r}_N$, $\vec{r}_p$ space.

Eqs. (1) and (7) imply that the difference between ψ_0 and ψ_D is everywhere outgoing. Rewriting eq. (6) as

$$(T_N + T_p + V_N - E)\psi_D = (V_N - V_{NP})\psi_D \tag{14}$$

it follows that [7]

$$\psi_D = \psi_0 + G(V_N - V_{NP})\psi_D \qquad (15)$$

so that eq. (7) becomes

$$\Psi = \psi_D - G(V_N - V_{NP})\psi_D - G(V_P + V_{NP})\Psi \qquad (16)$$

Eq. (16) is identical with Austern's integral equation[5].

Since V_{NP} does not appear in eq. (8), ψ_0 may be said to represent a combination of free space proton functions and of neutron functions $\varphi(r_N, \lambda)$, which at infinity looks like an incoming plane wave of free deuterons, but in which the neutrons and protons propagate independently of each other. In order that a neutron be captured it is necessary that the proton remove the excess neutron energy. But eq. (8) contains no neutron-proton coupling. Consequently it is to be expected that ψ_0 makes a vanishing contribution to the scattering amplitude, in (d,p) reactions.

This plausible argument can be made rigorous. Substitute eq. (16) in eq. (2). Using eq. (5) it is seen that the term in ψ_D vanishes exponentially as $r_p \to \infty$, since both Φ and φ are bound states. The terms in G simplify with the aid of eq. (10) and the orthonormality of the set $\varphi(\lambda)$. Letting $r_p \to \infty$, there results

$$A(\vec{n}) = A_1(\vec{n}) + A_2(\vec{n}) \tag{17}$$

$$A_1(\vec{n}) = -\frac{1}{4\pi}\frac{2M}{\hbar^2}\int d\vec{r}_p\, d\vec{r}_N\, e^{-i\vec{k}\cdot\vec{r}_p}\,\varphi^*(\vec{r}_N,\lambda_f)(V_N - V_{NP})\psi_D \tag{18}$$

$$A_2(\vec{n}) = -\frac{1}{4\pi}\frac{2M}{\hbar^2}\int d\vec{r}_p\, d\vec{r}_N\, e^{-i\vec{k}\cdot\vec{r}_p}\,\varphi^*(\vec{r}_N,\lambda_f)(V_p + V_{NP})\Psi \tag{19}$$

In eqs. (18) and (19) λ_f is the energy of the neutron in its final bound state, $\vec{k} = k\vec{n}$, and

$$\frac{\hbar^2 k^2}{2M} + \lambda_f = E = \frac{\hbar^2 K^2}{4M} + \epsilon \tag{20}$$

where, referring to eq. (5) ϵ is the energy of the deuteron in its ground state.

It can be shown that[7]

$$A_1(\vec{n}) = 0 \tag{21}$$

The demonstration is trivial, involves merely elimination of V_{NP} and V_N by eqs. (6) and (11) followed by an integration by parts. Eq. (21) remains valid when the particles are not assumed spinless, and when is not spherically symmetric, i.e. when V_{NP} is non-central and spin-dependent?

Eq. (21) means that, as asserted previously, $\psi_0 = \psi_D - G(V_N - V_{NP})\psi_D$ makes no contribution to the scattering amplitude. In Born approximation we replace Ψ by ψ_D in eq. (19). In this approximation, by virtue of eq. (18), we may replace V_{NP} by V_N, without additional error. This yields the starting point [2,3] for the Born approximation deductions of the (d,p) angular distribution. Our derivation may be compared with

Austern[5]. It will be noted that the valid use[2,3] of the Born approximation matrix element depends on the plausible but not obvious circumstance that ψ_0 makes no contribution to the scattering amplitude.

III Butler's Theory

Eq. (16) remains valid whatever the forms of V_P, V_N and V_{NP}, subject to the remark in footnote 9. The special assumptions made by Butler[1] may, for (d,p) reactions, be summarized as follows:[4] (a) $T_p = 0$; (b) within the nucleus, $r_N < a$, neglect V_{NP} in the Schroedinger equation for Ψ; (c) exterior to the nucleus, $r_N > a$, assume $V_N = 0$; (d) for $r_N > a$ Ψ is of the form eq. (1) where Φ is composed of free particles only, i.e. Φ satisfies, when $r_N > a$

$$(T_N + T_P - E)\Phi = 0 \tag{22}$$

We shall see that assumptions (c) and (d) are not entirely consistent. Assumptions (a), (b) and (c) mean the Schroedinger equation for the problem is

$$r_N < a \quad (T_N + T_P + V_N - E)\Psi = 0 \tag{23a}$$

$$r_N > a \quad (T_N + T_P + V_{NP} - E)\Psi = 0 \tag{23b}$$

Eqs. (23a) and (23b) may be expressed in the form, valid for all $\vec{r}_N$, $\vec{r}_P$

$$(T_N + T_P + V_N - E)\Psi = P_>(V_N - V_{NP})\Psi \tag{24}$$

where we have introduced the projection operator $P_>$

$$P_> = 0, \quad r_N < a \qquad P_> = 1, \quad r_N > a \tag{25}$$

The integral equation equivalent to eq. (24) is

$$\Psi = \psi_0 + G P_> (V_N - V_{NP}) \Psi = \psi_0 - G P_> V_{NP} \Psi \tag{26}$$

since $V_N = 0$ for $r_N > a$. As in the preceding section eq. (26) leads to the scattering amplitude

$$A(\vec{n}) = -\frac{1}{4\pi} \frac{2M}{\hbar^2} \int d\vec{r}_P \int_{r_N > a} d\vec{r}_N \, e^{-i\vec{k}_0 \cdot \vec{r}_P} \phi^*(\vec{r}_N, \lambda_f) \, V_{NP} \Psi \tag{27}$$

In Born approximation Ψ is replaced by ψ_D in eq. (27). Since the right side of eq. (24) can be interpreted as a source term, Born approximation in the theory of this section, i.e. Born approximation in eq. (24), amounts to neglecting as a source of scattered proton waves at infinity the term $V_{NP}\Psi$ exterior to the nucleus. But this is exactly the approximation which is implied by eq. (22), in which $V_{NP}\Psi$ is neglected for $r_N > a$. Consequently that Butler's solution[1] is equivalent to the Born approximation theory of this section is no longer surprising. In fact eq. (22) implies, using eqs. (1) and (6),

$$r_N > a \quad (T_N + T_P - E)\Psi = (T_N + T_P - E)\psi_D = -V_{NP}\psi_D \tag{28}$$

Eq. (28) may be rewritten as

$$r_N > a \quad (T_N + T_P + V_{NP} - E)\Psi = V_{NP}(\Psi - \psi_D) = V_{NP}\Phi \tag{29}$$

eq. (29) is not identical with eq. (23b).

It has been eqs. (23a) and (28) whose solutions have been fitted at the nuclear radius,[1,4,6] not eqs. (23a) and (23b). Recalling $V_N = 0$ for $r_N > a$, eqs. (23a) and (28) are equivalent to

$$(T_N + T_p + V_N - E)\Psi = -P_> V_{NP} \psi_D \qquad (30)$$

Eq. (30) is an inhomogeneous differential equation, not an integral equation, whose solution, satisfying the boundary conditions, is

$$\Psi = \psi_0 - G P_> V_{NP} \psi_D \qquad (31)$$

Eq. (31) is presumably the solution which is obtained by fitting the exterior and interior solutions at the nuclear radius. Comparing eqs. (26), (27), and (31), it is at once seen that the scattering amplitude in Butler's theory is the same as Born approximation in eq. (27), namely

$$A(\vec{n}) = -\frac{1}{4\pi}\frac{2M}{\hbar^2}\int d\vec{r}_p \int_{r_N > a} d\vec{r}_N\, e^{-i\vec{k}\cdot\vec{r}_p}\, \varphi^*(\vec{r}_N, \lambda_f) V_{NP} \psi_D \qquad (32)$$

Born approximation in eq. (19) reduces of course to eq. (32) if the additional assumptions involved in obtaining eq. (27) are included in eq. (19), namely, $V_p = 0$ and V_{NP} neglected for $r_N < a$.

IV Evaluation of Scattering Amplitude.

Eq. (32) must be integrated over the region $r_{II} > a$, and cannot be replaced by an integral over all space, even though we seemingly derived eq. (32) by neglecting V_{IIP} for $r_{II} < a$. V_{IIP} was neglected for $r_N < a$ in eq. (23a) only, which combined with eq. (28) led without further approximation to eq. (32). In eq. (4) for ψ_D no such assumption about V_{IIP} is made. Including in eq. (32) the region $r_{II} < a$ would amount to going back to the Born approximation of section II, but with $V_P = 0$.

As a consequence, it is not legitimate, in eq. (32), to replace V_{IIP} by V_N, since this substitution is justified only by eqs. (18) and (21) in which the integrals are extended over all space. That eq. (32) involves V_{IIP} rather than V_{II} is desirable, as it enables us to avoid such difficulties as those of Daitch and French[3] who obtain the angular distribution by neglecting the contribution from $r_{II} < a$ to the overlap integral between $\varphi^*(\vec{r}_{II}, \lambda_\varphi)$ and a spherical Bessel function. Because $\varphi(\vec{r}_{II}, \lambda_\varphi)$ is a bound state, decreasing exponentially for $r_{II} > a$, it is hard to justify their approximation.

We proceed now to evaluate $A(\vec{n})$ from eq. (32), to satisfy ourselves that it leads without further assumptions to Butler's angular distribution. The evaluation is straightforward and doubtless can be done in a number of ways. We have found it convenient to introduce in eq. (32) replacing $\vec{r}_P$ the new variable $\vec{r} = \vec{r}_P - \vec{r}_{II}$, and to make use of eq. (5) and the fact

that ψ_f is a function of $\vec{r}_N$ only, we have

$$A(\vec{n}) = -\frac{1}{4\pi}\frac{2M}{\hbar^2}\int d\vec{r}\, V_{NP}(r)\omega(r)e^{i\vec{r}\cdot(\vec{K}/2-\vec{k})}\int_{r_N>a} d\vec{r}_N\, e^{i\vec{r}_N\cdot(\vec{K}-\vec{k})}\varphi^*(\vec{r}_N,\lambda_f) \tag{33}$$

In the integral over $\vec{r}$ in eq. (33) use

$$\left[-\frac{\hbar^2}{M}\Delta_r + V_{NP}(r)\right]\omega(r) = \epsilon\,\omega(r) \tag{34}$$

to eliminate V_{NP}, integrate by parts, justified because ω is a bound state, and employ eq. (20), obtaining

$$\int d\vec{r} V_{NP}\omega e^{i\vec{r}\cdot(\vec{K}/2-\vec{k})} = \left[\lambda_f - \frac{\hbar^2}{2M}(\vec{K}-\vec{k})^2\right]\int d\vec{r}\,\omega\, e^{i\vec{r}\cdot(\vec{K}/2-\vec{k})} \tag{35}$$

From eq. (11) for $r_N > a$, where $V_N = 0$,

$$\left[\lambda_f - \frac{\hbar^2}{2M}(K-k)^2\right]e^{i\vec{r}_N\cdot(\vec{K}-\vec{k})}\varphi^*(\vec{r}_N,\lambda_f) = -\frac{\hbar^2}{2M}\left[e^{i\vec{r}_N\cdot(\vec{K}-\vec{k})}\Delta\varphi^* - \varphi^*\Delta e^{i\vec{r}_N\cdot(\vec{K}-\vec{k})}\right] \tag{36}$$

Hence, using Green's theorem in the integral over $\vec{r}_N$, expanding $e^{i\vec{r}_N\cdot(\vec{K}-\vec{k})}$ in spherical harmonics with $\vec{K}-\vec{k}$ as the polar axis, and writing $\varphi = R_\ell(r_N)\,Y_\ell^m(\theta_N,\phi_N)$, eqs. (33) - (36) imply

$$A(n) = -i^\ell(2\ell+1)^{\frac{1}{2}}a^2\left[j_\ell(|\vec{K}-\vec{k}|r_N)\frac{\partial R_\ell}{\partial r_N} - R_\ell\frac{\partial}{\partial r_N}j_\ell(|\vec{K}-\vec{k}|r_N)\right]_{r_N=a}\int d\vec{r}\,\omega(r)e^{i\vec{r}\cdot(\vec{K}-\vec{k})} \tag{37}$$

Eq. (37) is valid for $m=0$, with $Y_\ell^m(\theta_N,\phi_N)$ quantized along $\vec{K}-\vec{k}$. The integral vanishes for the other values of the magnetic quantum number. Eq. (37) yields Butler's angular distribution, as has been previously[3] pointed out.

V. Success of the Theory

It appears established that Butler's theory accounts for the observed angular distributions in (d,p) reactions. The success of the theory remains surprising, in view of the relatively low energy deuterons which have been used in the experiments. We have seen that Butler's assumption (d), section III, is equivalent to neglecting as a source of proton waves the term $V_{NP}\Phi$ exterior to the nucleus, and that this neglect is identical with Born approximation. It is well known that Born approximation is often much better than expected; the theory of angular distributions in (d,p) reactions seems to be another such case, and we offer no explanation.

Assumption (b), section III, led to eq. (32) being integrated over $r_N > a$ rather than over all space, as in eq. (19). In a sense neglect of V_{NP} for $r_N < a$ can be thought of as an impulse approximation, i. e. the neutron-proton forces do not have time to act in the interval that the deuteron overlaps the nucleus. But this interpretation is hard to justify, since V_{NP} is not smaller than V_N, and since the deuterons are slow. In any event it is difficult to see why neglect of V_{NP} for $r_N < a$ should lead to a better result than including it. Integrating over all r_N in eq. (32) permits V_{NP} to be replaced by V_N, as we have seen, and leads to a modified angular distribution[3] which, however, is generally not very different from Butler's original form. It is doubtful that the available data are accurate enough to choose between the two possibilities:

integrating over $r_N > a$ and integrating over all r_P. With better data on selected nuclei in which the differences between the two forms are emphasized, together with comparisons of absolute cross sections with the theory, a decision between the two alternatives may be feasible.

An alternative means (to that in section III) of converting the Schroedinger equation of the problem to an inhomogeneous differential equation is to replace the assumptions (a) - (d) of section III by: (a') $V_P = 0$; (b') assume $V_N = 0$ for $r_N > a$; (c') for $r_N < a$ Ψ satisfies

$$r_N < a \qquad (T_N + T_P + V_{NP} - E)\Psi = -V_N \psi_D \tag{38}$$

With these assumptions V_{NP} is nowhere neglected.

If ψ_D is replaced by Ψ on the right side of eq. (38) we obtain the presumably correct eq. (4), with of course $V_P = 0$. Thus eq. (38) amounts to neglecting $V_N \Phi$ as a source term, in the region $r_N < a$.

Without going into as many details as previously, assumptions (a') - (c') imply the solution Ψ is

$$\Psi \equiv \psi_D - G_1 V_N \psi_D \tag{39}$$

where G_1 is the outgoing Green's function satisfying

$$(T_N + T_P + V_{NP} - E)G_1 = 1 \tag{40}$$

To determine the scattering amplitude in closed form we must express G_1 in terms of G, eq. (9), enabling us to employ the orthonormality of the set $\varphi(\lambda)$. From eq. (40) the integral

equation for G_1 is

$$G_1 = G + G(V_N - V_{NP})G_1 \tag{41}$$

Substituting eq. (41) in eq. (39) the scattering amplitude $A(\vec{n})$ is seen to be

$$A(\vec{n}) = -\frac{1}{4\pi}\frac{2M}{\hbar^2}\int d\vec{r}_N\, d\vec{r}_p\, e^{-i\vec{k}\cdot\vec{r}_p}\varphi^*(\vec{r}_N, \lambda_f)\, V_N\, \psi_D$$

$$-\frac{1}{4\pi}\frac{2M}{\hbar^2}\int d\vec{r}_N\, d\vec{r}_p\, d\vec{r}_N'\, d\vec{r}_p'\, e^{-i\vec{k}\cdot\vec{r}_p}\varphi^*(\vec{r}_N, \lambda_f)\left[V_N(\vec{r}_N) - V_{NP}(\vec{r}_p - \vec{r}_N)\right] G(\vec{r}_N, \vec{r}_N'; \vec{r}_p, \vec{r}_p')\, V_N(\vec{r}_N')\, \psi_D(\vec{r}_N', \vec{r}_p') \tag{42}$$

Eq. (42) can be approximated by ignoring the term in $G_1\ V_N \underset{\sim}{\psi}_D = \psi_D - \Phi$, e. g. (39), which vanishes in Born approximation $\Psi = \psi_D$. In first approximation therefore $A(\vec{n})$ of eq. (42) is identical with the Born approximation to eq. (19) with $V_p = 0$. Other equally reasonable ways of estimating eq. (42) lead to the same conclusion.

The above discussion demonstrates that a variety of different approaches can lead to angular distributions resembling Butler's. This helps to make understandable the success of his theory in accounting for obersved angular distributions. As a corollary, the success of Butler's theory with presently available data does not strongly support his particular model.

We consider the physics of the (d,p) reaction still somewhat obscure, and until this is better elucidated we see no good reason why Butler's original formula eq. (32) should be superior to say Born approximation in eq. (19) or to eq. (42) including the second correction term.

We add that it seems possible to carry through the calculations of this paper including spin and without making the approximation that the nucleus is a center of force. By this means we would arrive at the selection rules[1], but would not otherwise add enough to the simpler theory we have presented to warrant the extra formal complications. The chief desideratum of a more careful discussion would be to arrive at an improved estimate of the magnitude of the cross section, [1,2,4,6] but this we are not yet prepared to do.